**Table 4.** Proteins that exhibit significantly decreased expression in specimen of microdissected glomerular cross sections from diabetic patients with diabetic nephropathy and their cellular locations

| Protein name | GI number | Fold change Versus non-diabetic glomeruli | P-value | Location |
|---|---|---|---|---|
| Renal and urological disease-related proteins | | | | |
| Myosin, heavy chain 9, non-muscle | 6166599 | 0.89 | 0.0001 | Cytoplasm |
| Gelsolin | 121116 | 0.89 | 0.0098 | Extracellular space |
| Clathrin, heavy chain | 1705916 | 0.86 | 0.0231 | Plasma membrane |
| Actinin, alpha 4 | 13123943 | 0.81 | 0.0001 | Cytoplasm |
| Tubulin, alpha 1c | 20455322 | 0.78 | 0.0018 | Cytoplasm |
| S100 calcium-binding protein A6 | 116509 | 0.76 | 0.0001 | Cytoplasm |
| Carbonic anhydrase I | 115449 | 0.76 | 0.0087 | Cytoplasm |
| Immunoglobulin heavy constant gamma 1 | 121039 | 0.75 | 0.0001 | Extracellular space |
| Carbonic anhydrase II | 115456 | 0.75 | 0.0001 | Cytoplasm |
| Membrane metallo-endopeptidase | 128062 | 0.70 | 0.0258 | Plasma membrane |
| Podocin | 12230467 | 0.70 | 0.0055 | Plasma membrane |
| Other proteins | | | | |
| Actin, beta-like 2 | 172046825 | 0.94 | 0.0005 | Unknown |
| Spectrin, alpha, non-erythrocytic 1 | 94730425 | 0.93 | 0.0422 | Plasma membrane |
| Peroxiredoxin 1 | 548453 | 0.93 | 0.0266 | Cytoplasm |
| Heat shock 70-kDa protein 5 | 14916999 | 0.93 | 0.0333 | Cytoplasm |
| Aminoacylase 1 | 461466 | 0.92 | 0.0419 | Cytoplasm |
| Lamin A/C | 125962 | 0.91 | 0.0024 | Nucleus |
| ATP synthase, beta polypeptide | 114549 | 0.90 | 0.0259 | Cytoplasm |
| Calmodulin-like 3 | 115502 | 0.89 | 0.0293 | Cytoplasm |
| Myosin, heavy chain 9, non-muscle | 6166599 | 0.89 | 0.0001 | Cytoplasm |
| Phosphoglycerate kinase 2 | 21264485 | 0.87 | 0.0058 | Cytoplasm |
| Annexin A2 pseudogene 2 | 205830271 | 0.87 | 0.0016 | Unknown |
| Moesin | 127234 | 0.87 | 0.0004 | Plasma membrane |
| Peroxiredoxin 6 | 1718024 | 0.86 | 0.0095 | Cytoplasm |
| Heterogeneous nuclear ribonucleoprotein A2/B1 | 133257 | 0.86 | 0.009 | Nucleus |
| Dihydropyrimidinase-like 3 | 3122050 | 0.85 | 0.009 | Cytoplasm |
| Histone cluster 3, H3 | 18202512 | 0.84 | 0.0016 | Nucleus |
| Histone cluster 1, H1c | 417101 | 0.83 | 0.0004 | Nucleus |
| Malate dehydrogenase 2, NAD | 215274114 | 0.82 | 0.0071 | Cytoplasm |
| Myosin, light chain 6B | 127153 | 0.81 | 0.0035 | Cytoplasm |
| Alpha-2-macroglobulin | 269849533 | 0.78 | 0.0247 | Extracellular space |
| Reticulon 4 | 17369290 | 0.78 | 0.0056 | Cytoplasm |
| H2A histone family, member X | 121992 | 0.76 | 0.0001 | Nucleus |
| Tubulin, beta 8 | 182705285 | 0.75 | 0.0001 | Unknown |
| Solute carrier family 9 member 3 regulator 2 | 42559433 | 0.74 | 0.0183 | Plasma membrane |
| Protease, serine, 2 (trypsin 2) | 136413 | 0.74 | 0.0004 | Extracellular space |
| Cysteine and glycine-rich protein 1 | 118161 | 0.74 | 0.0036 | Nucleus |
| Transferrin | 136191 | 0.73 | 0.0001 | Extracellular space |
| Vimentin | 55977767 | 0.72 | 0.0001 | Cytoplasm |
| Nestin | 146345464 | 0.69 | 0.0001 | Cytoplasm |
| PDZ and LIM domain 2 | 67461069 | 0.69 | 0.0001 | Cytoplasm |
| IQ motif-containing GTPase-activating protein 2 | 292495090 | 0.67 | 0.0009 | Cytoplasm |
| Tubulin polymerization-promoting protein family member 3 | 28380040 | 0.60 | 0.0002 | Unknown |
| Hemoglobin, delta | 122713 | 0.48 | 0.0001 | Cytoplasm |
| Hemoglobin, zeta | 122335 | 0.47 | 0.0001 | Cytoplasm |

between the numerical fraction of nephronectin-positive glomerular cross sections and the histological glomerular sclerosis index ($\rho = 0.881$, $P < 0.0001$, $n = 93$). There was a significant positive correlation between these parameters in diabetic patients with and without nephropathy ($\rho = 0.889$, $P < 0.0001$ and 0.699, $P < 0.0001$, respectively, Table 5). There was no significant correlation between these measures in non-diabetic patients ($\rho = 0.134$, $P = 0.707$).

## Discussion

The present study implemented proteomic analysis of laser microdissected glomeruli from FFPE kidneys of autopsies of diabetic patients with nephropathy and non-diabetic patients using QSTAR Elite LC–MS/MS and iTRAQ technology identified 100 proteins that were differentially expressed. Among these proteins, 31 renal and urological disease-related proteins were detected. Nephronectin is one of the renal and urological disease-related proteins that were significantly overexpressed in samples of microdissected glomerular cross sections from diabetic patients with nephropathy. Immunohistochemical analysis demonstrated that glomerular nephronectin immunoreactivity was positive in diabetic patients in subjects with and without nephropathy, and was particularly positive in those with nephropathy, but negative in non-diabetic patients.

Downloaded from http://ndt.oxfordjournals.org/ at Osaka City University on December 16, 2011

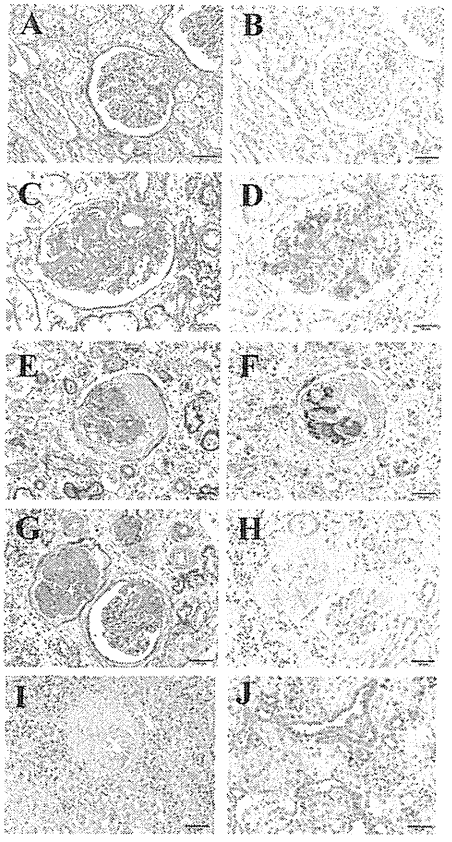


**Fig. 3.** Periodic acid-Schiff (**A**, **C**, **E**, **G**) and nephronectin staining (**B**, **D**, **F**, **H**, **I**, **J**) in the autopsy kidneys from non-diabetic patients (A, B), diabetic patients (C, D, E, F, G, H, I) and mice (J): nephronectin immunoreactivity was negative in normal glomeruli but was positive in tubular epithelial cells in kidneys from the non-diabetic patients (A, B). Nephronectin immunoreactivity was positive in areas of diffuse mesangial expansion in diabetic patients (C, D). Nephronectin immunoreactivity was positive in areas of nodular glomerulosclerosis in diabetic patients (E, F). Nephronectin immunoreactivity was weakly positive in areas of glomerular exudative changes in diabetic nephropathy patients (G, H). No immunoreactive staining was observed in negative control specimens from the diabetic patients (I). Nephronectin immunoreactivity was positive in tubular epithelial cells of mouse kidney sections as positive controls (J). Scale bar indicates 50 μm.

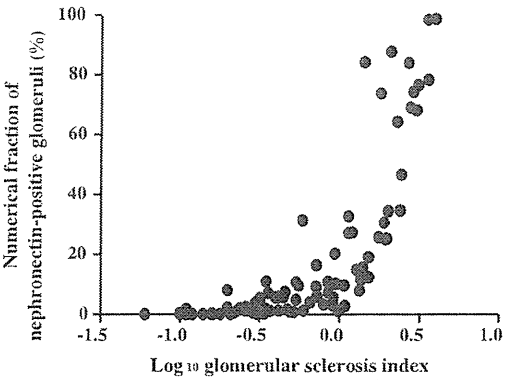


**Fig. 4.** Correlation analysis of the numerical fraction of nephronectin-positive glomerular cross sections and the histological glomerular sclerosis index in diabetic patients with and without nephropathy. There was a significant positive correlation between the numerical fraction of nephronectin-positive glomerular cross sections and the glomerular sclerosis index. ($\rho = 0.881$, $n = 93$).

Concerning the glomerular alterations in diabetic nephropathy, nodular glomerulosclerosis has been suggested to be a progressive form of diffuse mesangial expansion via a mesangiolytic step [24] that is specific to diabetic glomeruli. Mesangial expansion occurs due to the accumulation of extracellular matrix in the mesangium as a result of augmented deposition of extracellular matrix protein [25, 26]. Nephronectin has been reported to be associated with the assembly of extracellular matrix [27–29] and plays a crucial role during early metanephric kidney development [21, 22]. The findings of highly expressed nephronectin in glomeruli from diabetic patients with and without nephropathy but not in those from non-diabetic patients and the significant positive correlation between the numerical fraction of nephronectin-positive glomerular cross sections and the histological glomerular sclerosis index in diabetic patients both with and without nephropathy suggest that nephronectin is associated with the development of diabetic glomerulosclerosis and consequent nephropathy. Furthermore, the glomerular nephronectin immunoreactivity was also increased significantly in the glomeruli from diabetic patients without nephropathy compared with non-diabetic patients, despite the fact that there were no significant differences in the glomerular sclerosis index between these groups. This suggests that nephronectin may also be involved in the early stages of the development of glomerulosclerosis.

As mentioned above, nephronectin is associated with the assembly of extracellular matrix [27–29] and the accumulation of extracellular matrix in the mesangium is due to the augmented deposition of extracellular matrix protein, such as collagen Types I, IV, V, VI, laminin and fibronectin [25, 26]. In the current proteome analysis, collagen Types IV, VI, laminin and fibronectin were also overexpressed in glomerular cross sections from diabetic patients with nephropathy. These findings provide further evidence for the above notion that nephronectin is related to the diabetic glomerular alterations of diffuse mesangial expansion and nodular glomerulosclerosis. Although exudative lesions are often seen in diabetic kidneys, they are not specific to diabetic nephropathy and also appear to be due to increases in plasma lipoprotein [30]. In the present study, glomerular nephronectin immunoreactivity was positive in some exudative lesions, but was weakly positive, compared with strong immunoreactivity in diffuse mesangial expansion. This suggests that nephronectin is predominantly involved in the development of diffuse mesangial expansion and nodular glomerulosclerosis and that the levels of nephronectin may more appropriately reflect the status of diabetic nephropathy.

To the best of our knowledge, the present study is the first proteome analysis to use laser microdissected glomeruli from FFPE kidney tissues of diabetic nephropathy from human autopsy cases. In addition to nephronectin, apolipoprotein E is a well-known protein related to diabetic nephropathy [12, 31], which we observed to also be significantly overexpressed in glomerular cross sections from diabetic

Downloaded from http://ndt.oxfordjournals.org/ at Osaka City University on December 16, 2011

**Table 5.** Histopathological analysis of diabetic patients with and without nephropathy and non-diabetic patients[a]

| | Diabetic patients | | |
|---|---|---|---|
| | With nephropathy ($n$ = 45) | Without nephropathy ($n$ = 48) | Non-diabetic patients ($n$ = 10) |
| Numerical fraction of nephronectin-positive glomerular cross sections (%) | 32.1 ± 31.5* | 4.14 ± 5.65**,*** | 0.54 ± 0.36 |
| Glomerular sclerosis index | 1.51 ± 1.01* | 0.44 ± 0.35**,**** | 0.25 ± 0.17 |
| $\rho$***** (P-values) | $\rho$ = 0.889 (P < 0.0001) | $\rho$ = 0.699 (P < 0.0001) | $\rho$ = 0.134 (P = 0.707) |

[a]The data are expressed as the mean ± SD.
*P < 0.0001 versus non-diabetic patients.
**P < 0.0001 versus with nephropathy.
***P < 0.0001 versus non-diabetic patients.
****P = 0.073 versus non-diabetic patients.
*****Correlation coefficients between the numerical fraction of nephronectin-positive glomerular cross sections and the glomerular sclerosis index.

patients with nephropathy in the present study. Consistent with a previous report [32], collagen Type IV, an extracellular matrix protein that accumulates in sclerotic areas of diabetic glomeruli, was also overexpressed in the present study. The results of immunohistochemistry of apolipoprotein E and collagen Type IV were clearly positive in glomeruli from diabetic patients with nephropathy (Supplementary file). Furthermore, we also found that alpha-actinin-4 and podocin, which are related to podocyte injury and proteinuria [33, 34], exhibited reduced expression in diabetic patients with nephropathy. Therefore, it is reasonable to consider that the results of our proteome analysis reflected glomerular alterations of diabetic glomeruli to a great extent. We consider that nephronectin is thus demonstrated to be one of the proteins that are altered in glomeruli of patients with diabetic nephropathy. Our results also demonstrate the usefulness of proteome analysis of laser microdissected glomeruli from FFPE kidney tissues from autopsy patients in investigations of the molecular mechanisms of diabetic nephropathy. Although using microdissected glomerular samples from FFPE kidney tissues from autopsy material may reduce the detection of proteins compared with frozen tissue biopsies, the method in the present study enabled us to collect sufficient amounts of glomerular tissue. Since renal biopsy is clinically limited for diabetic patients and since sufficient quantities of renal biopsy specimens are not usually available for proteome analysis, we provide a new approach for investigations of renal disease, including diabetic nephropathy.

Recently, urinary-based proteome analyses of diabetic nephropathy have identified some proteins, such as collagen Type I, as candidate urinary biomarkers of diabetic nephropathy [7–9]. Proteome analysis of serum specimens from Type 2 diabetes patients has also shown that vitamin D-binding protein may be employed as a diagnostic and monitoring biomarker of microalbuminuria [10] and that extracellular glutathione peroxidase and apolipoprotein E may constitute potential biomarkers for the diagnosis of Type 2 diabetes with nephropathy [11]. However, expression of the above mentioned proteins in the kidneys from diabetic patients with nephropathy has not been investigated. Apart from apolipoprotein E, these proteins were not detected in the glomerular samples in the present study. The differences in the findings between the present study and the above urinary and serum studies could be attributed to differences in the samples examined and methods employed. The urine and serum levels of nephronectin were not examined in the present study due to the fact that urine and serum samples were not available from the autopsy cases investigated.

In conclusion, the present study demonstrated, for the first time, that nephronectin may be associated with the development of diabetic glomerulosclerosis and that proteome analysis of FFPE kidney tissues from diabetic patients with nephropathy is a useful tool for understanding diabetic nephropathy. Further studies with serum and urine are needed to evaluate the usefulness of nephronectin as a new biomarker that reflects glomerular alterations in diabetic nephropathy. Further studies are also needed to examine the role of nephronectin in other types of proliferative mesangial glomerulonephritis, such as IgA glomerulonephritis. Immunohistochemical staining of biopsy specimens obtained from living diabetic patients or from tumor nephrectomy tissues will be necessary for further proof of our findings.

## Supplementary data

Supplementary file is available online at http://ndt.oxfordjournals.org.

*Acknowledgements.* We thank Mr Shotaro Yamano, Ms Kaori Touma, Ms Azusa Inagaki and Ms Rie Onodera for their technical assistance and Ms Yukiko Iura for her assistance in the preparation of this manuscript. This work was supported by a Grant-in-Aid for Scientific Research of The Ministry of Education, Culture, Sports, Science and Technology of Japan (#23591198).

*Conflict of interest statement.* None declared.

## References

1. Collins AJ, Foley RN, Herzog C *et al.* United States Renal Data System 2008 Annual Data Report. *Am J Kidney Dis* 2009; 53 (1 Suppl): S1–S374
2. Caramori ML, Fioretto P, Mauer M. Enhancing the predictive value of urinary albumin for diabetic nephropathy. *J Am Soc Nephrol* 2006; 17: 339–352

Downloaded from http://ndt.oxfordjournals.org/ at Osaka City University on December 16, 2011

3. Hovind P, Tarnow L, Rossing K *et al.* Decreasing incidence of severe diabetic microangiopathy in type 1 diabetes. *Diabetes Care* 2003; 26: 1258–1264
4. Wild S, Roglic G, Green A *et al.* Global prevalence of diabetes: estimates for the year 2000 and projections for 2030. *Diabetes Care* 2004; 27: 1047–1053
5. Anderson NL, Anderson NG. The human plasma proteome: history, character, and diagnostic prospects. *Mol Cell Proteomics* 2002; 1: 845–867
6. Akkina SK, Zhang Y, Nelsestuen GL *et al.* Temporal stability of the urinary proteome after kidney transplant: more sensitive than protein composition? *J Proteome Res* 2009; 8: 94–103
7. Otu HH, Can H, Spentzos D *et al.* Prediction of diabetic nephropathy using urine proteomic profiling 10 years prior to development of nephropathy. *Diabetes Care* 2007; 30: 638–643
8. Gu W, Zou LX, Shan PF *et al.* Analysis of urinary proteomic patterns for diabetic nephropathy by ProteinChip. *Proteomics Clin Appl* 2008; 2: 744–750
9. Rossing K, Mischak H, Dakna M *et al.* Urinary proteomics in diabetes and CKD. *J Am Soc Nephrol* 2008; 19: 1283–1290
10. Cho EH, Kim MR, Kim HJ *et al.* The discovery of biomarkers for type 2 diabetic nephropathy by serum proteome analysis. *Proteomics Clin Appl* 2007; 1: 352–361
11. Kim HJ, Cho EH, Yoo JH *et al.* Proteome analysis of serum from type 2 diabetics with nephropathy. *J Proteome Res* 2007; 6: 735–743
12. Guan J, Zhao HL, Baum L *et al.* Apolipoprotein E polymorphism and expression in type 2 diabetic patients with nephropathy: clinicopathological correlation. *Nephrol Dial Transplant* 2009; 24: 1889–1895
13. Xu H, Yang L, Wang W *et al.* Antigen retrieval for proteomic characterization of formalin-fixed and paraffin-embedded tissues. *J Proteome Res* 2008; 7: 1098–1108
14. Kakehashi A, Ishii N, Shibata T *et al.* Mitochondrial prohibitins and septin 9 are implicated in the onset of rat hepatocarcinogenesis. *Toxicol Sci* 2011; 119: 61–72
15. Hill EG, Schwacke JH, Comte-Walters S *et al.* A statistical model for iTRAQ data analysis. *J Proteome Res* 2008; 7: 3091–3101
16. Wang YS, Cao R, Jin H *et al.* Altered protein expression in serum from endometrial hyperplasia and carcinoma patients. *J Hematol Oncol* 2011; 4: 15–22
17. Shilov IV, Seymour SL, Patel AA *et al.* The Paragon Algorithm, a next generation search engine that uses sequence temperature values and feature probabilities to identify peptides from tandem mass spectra. *Mol Cell Proteomics* 2007; 6: 1638–1655
18. Sui J, Zhang J, Tan TL *et al.* Comparative proteomics analysis of vascular smooth muscle cells incubated with S- and R-enantiomers of atenolol using iTRAQ-coupled two-dimensional LC-MS/MS. *Mol Cell Proteomics* 2008; 7: 1007–1018
19. Ma LJ, Nakamura S, Whitsitt JS *et al.* Regression of sclerosis in aging by an angiotensin inhibition-induced decrease in PAI-1. *Kidney Int* 2000; 58: 2425–2436
20. Liu X, Lu L, Tao BB *et al.* Amelioration of glomerulosclerosis with all-trans retinoic acid is linked to decreased plasminogen activator inhibitor-1 and alpha-smooth muscle actin. *Acta Pharmacol Sin* 2011; 32: 70–78
21. Brandenberger R, Schmidt A, Linton J *et al.* Identification and characterization of a novel extracellular matrix protein nephronectin that is associated with integrin alpha8beta1 in the embryonic kidney. *J Cell Biol* 2001; 154: 447–458
22. Miner JH. Mystery solved: discovery of a novel integrin ligand in the developing kidney. *J Cell Biol* 2001; 154: 257–259
23. Cheng CW, Ka SM, Yang SM *et al.* Nephronectin expression in nephrotoxic acute tubular necrosis. *Nephrol Dial Transplant* 2008; 23: 101–109
24. Kida H, Yoshimura M, Ikeda K *et al.* Pathogenesis of diabetic nephropathy in non-insulin-dependent diabetes mellitus. *J Diabet Complications* 1991; 5: 82–83
25. Suzuki D, Miyazaki M, Jinde K *et al.* In situ hybridization studies of matrix metalloproteinase-3, tissue inhibitor of metalloproteinase-1 and type IV collagen in diabetic nephropathy. *Kidney Int* 1997; 52: 111–119
26. Schena FP, Gesualdo L. Pathogenetic mechanisms of diabetic nephropathy. *J Am Soc Nephrol* 2005; 16 (Suppl 1): S30–S33
27. Hynes RO. Integrins: bidirectional, allosteric signaling machines. *Cell* 2002; 110: 673–687
28. Takagi J. Structural basis for ligand recognition by integrins. *Curr Opin Cell Biol* 2007; 19: 557–564
29. Sato Y, Uemura T, Morimitsu K *et al.* Molecular basis of the recognition of nephronectin by integrin alpha8beta1. *J Biol Chem* 2009; 284: 14524–14536
30. Hall GF. The significance of atheroma of the renal arteries in Kimmelstiel-Wilson's syndrome. *J Pathol Bacteriol* 1952; 64: 103–120
31. Lassila M, Seah KK, Allen TJ *et al.* Accelerated nephropathy in diabetic apolipoprotein e-knockout mouse: role of advanced glycation end products. *J Am Soc Nephrol* 2004; 15: 2125–2138
32. Nangaku M, Izuhara Y, Usuda N *et al.* In a type 2 diabetic nephropathy rat model, the improvement of obesity by a low calorie diet reduces oxidative/carbonyl stress and prevents diabetic nephropathy. *Nephrol Dial Transplant* 2005; 20: 2661–2669
33. Michaud JL, Chaisson KM, Parks RJ *et al.* FSGS-associated alpha-actinin-4 (K256E) impairs cytoskeletal dynamics in podocytes. *Kidney Int* 2006; 70: 1054–1061
34. Ikezumi Y, Suzuki T, Karasawa T *et al.* Activated macrophages down-regulate podocyte nephrin and podocin expression via stress-activated protein kinases. *Biochem Biophys Res Commun* 2008; 376: 706–711

*Received for publication: 2.6.11; Accepted in revised form: 28.10.11*

Downloaded from http://ndt.oxfordjournals.org/ at Osaka City University on December 16, 2011

TOXICOLOGICAL SCIENCES 126(1), 39–51 (2012)
doi:10.1093/toxsci/kfs016
Advance Access publication January 16, 2012

# Hormonally Active Doses of Isoflavone Aglycones Promote Mammary and Endometrial Carcinogenesis and Alter the Molecular Tumor Environment in Donryu Rats

Anna Kakehashi,* Yoshiyuki Tago,* Midori Yoshida,† Yui Sokuza,* Min Wei,* Shoji Fukushima,*,[1] and Hideki Wanibuchi*,[2]

*Department of Pathology, Osaka City University Graduate School of Medicine, 1-4-3 Asahi-machi, Abeno-ku, Osaka 545-8585, Japan; and †Division of Pathology, Biological Safety Research Center, National Institute of Health Sciences, Ministry of Health, Labour and Welfare, 1-18-1 Kamiyoga, Setagaya-ku, Tokyo 158-8501, Japan

[1]Present address: Japan Bioassay Research Center, 2445 Hirasawa, Hadano, Kanagawa 257-0015, Japan.
[2]To whom correspondence should be addressed. Fax: +81-6-6646-3093. E-mail: wani@med.osaka-cu.ac.jp.

Received October 17, 2011; accepted December 12, 2011

**Our research is focused on modifying effects of an isoflavone aglycones (IAs)-rich extract at a hormonally active dose of 150 mg/kg body weight/day on mammary and endometrial carcinogenesis in female Donryu rats. IA administered for 2 weeks in a phytoestrogen-low diet exerted estrogenic activity and induced cell proliferation in the uterus of ovariectomized rats. Furthermore, administration for 4 weeks resulted in elevation of cell proliferation in the mammary glands of 7,12-dimethylbenz[a] anthracene (DMBA)-treated animals. Forty weeks of postpubertal administration of IA to 5-week-old rats after initiation of mammary and endometrial carcinogenesis with DMBA and N-ethyl-N′-nitro-N-nitrosoguanidine (ENNG) caused significant increase of incidence and multiplicity of mammary adenocarcinoma, multiplicities of endometrial atypical hyperplasia, adenomatous polyps, and an increased trend of uterine adenocarcinomas. Liquid chromatography with tandem mass spectrometry and immunohistochemical analyses revealed significant elevation of tumorigenesis-related proteins such as S100 calcium-binding protein A8, kininogen 1, and annexins 1 and 2 in mammary adenocarcinomas and cadherin EGF LAG seven-pass G-type receptor 2, DEAD box polypeptide 1, and cysteine- and glycine-rich protein 1 in uterine proliferative lesions of IA-treated animals. Those changes are likely to be related to modulation of estrogen receptor (ER), AP1, nuclear factor-kappa B, and actin signaling pathways. Our results indicate that the postpubertal exposure of Donryu rats to IA at an estrogenic dose results in promotion of mammary and uterine carcinogenesis induced by DMBA and ENNG, which might be related to the activation of ER-dependent signaling and alteration of the molecular tumor environment in the mammary gland and endometrium.**

*Key Words:* mammary gland; uterus; isoflavone aglycones; estrogen; rat.

Isoflavone aglycones (IAs) found in soy products, like genistein, daidzein, and glycitein, are phytochemicals with various biological activities. Recently, more and more data have appeared demonstrating that the purported health benefits of soy isoflavones are quite variable, and the proposed protection offered by consumption is controversial (Banerjee *et al.*, 2008; Xiao, 2008). It has been shown that soy-derived isoflavones, which exhibit estrogen-like properties under certain experimental conditions, may stimulate the growth of existing estrogen-sensitive breast tumors (Messina and Loprinzi, 2001). Furthermore, it has been reported that isoflavones bind and transactivate estrogen receptors (ERs) (Jefferson and Newbold, 2000). Nanomolar concentrations of genistein were further shown to induce acid ceramidase (ASAH1) transcription through a GPR30-dependent pertussis toxin-sensitive pathway that requires the activation of c-Src and extracellular signal-regulated kinase 1/2 (ERK1/2), thus stimulating breast cancer cell growth (Lucki and Sewer, 2011).

On the basis of findings of a clinical trial performed using 179 postmenopausal women with intact uteri treated with 150 mg of isoflavones over a period of 5 years (Unfer *et al.*, 2004a), it was concluded that the long-term treatment (up to 5 years) with soy phytoestrogens (40–45% genistein [G], 40–45% daidzein [D], and 10–20% glycitein [Gl]; G:D:Gl = 2:2:1) was associated with an increased occurrence of endometrial hyperplasia. These findings call into question the safety of a long-term application of phytoestrogens with regard to the endometrium. However, *in vivo* data about the influence of soy isoflavones on uterine carcinogenesis are very limited. In rats, the incidences of spontaneous endometrial carcinomas are generally low, and only a few attempts at experimental induction of uterine adenocarcinoma by chemicals and/or hormones have been successful. Therefore, it has been difficult to assess the effects of any compound on uterine carcinogenesis in this animal species. To overcome this problem, a unique model for endometrial adenocarcinoma development has been established using the Donryu strain. A hormonal imbalance in this rat strain is associated with spontaneous endometrial adenocarcinoma

© The Author 2012. Published by Oxford University Press on behalf of the Society of Toxicology. All rights reserved.
For permissions, please email: journals.permissions@oup.com

Downloaded from http://toxsci.oxfordjournals.org/ at Oska City University - Medical Campus on February 28, 2012

development at 2 years of age (Maekawa *et al.*, 1986; Nagaoka *et al.*, 1990, 1994). Furthermore, high yields of uterine cancers can be induced by intrauterine administration of N-ethyl-N'-nitro-N-nitrosoguanidine (ENNG) via the vagina (Yoshida *et al.*, 1998).

Older adults in Asia were reported to consume approximately 6–11 g of soy protein and 25–80 mg of isoflavones (expressed as aglycone equivalents) per day. In contrast, people in the United States and Europe consume on average less than 3 mg/day of isoflavones (Messina and Wood, 2008). However, nowadays, many people are taking isoflavones as supplements. From the results of Unfer *et al.* (2004a) showing induction of uterine endometrial hyperplasia with an intake of 150 mg/day and the existing possibility that high concentrations of soy isoflavones might be hormonally active and exert adverse effects on hormonal carcinogenesis, in 2006, the Ministry of Health, Labour and Welfare of Japan has accepted 75 mg/day intake (acceptable daily intake [ADI]) of soybean isoflavone to be the safe level for humans (Unfer *et al.*, 2004a,b).

It is of particular importance to detect whether hormonally active concentrations of isoflavones, especially IAs free of soy protein that are used now as supplements, might exert promoting effects on hormonal carcinogenesis. Therefore, the present study was carried out to investigate the influence of IA (genistein [52%], daidzein [42%], and glycitein [6%]) at an estrogenic dose on mammary and uterine endothelial carcinogenesis after initiation using the Donryu rat model.

## MATERIALS AND METHODS

***Chemicals.*** 7,12-Dimethylbenz[a]anthracene (DMBA) was obtained from Tokyo Chemical Industry Co. Ltd, Tokyo, Japan, and ENNG from Nacalai Tesque, Kyoto, Japan. Polyethylene glycol (PEG) was from Wako Pharmaceutical, Osaka, Japan. Other chemicals were purchased from Sigma Chemical and were of analytical high performance liquid chromatography grade.

***IA-rich extract.*** The IA-rich extract (SoyAct) was provided by Kikkoman Corporation (Noda City, Chiba, Japan). The extract was produced by fermentation of soy followed by ethanol/water extraction and purification and contained IAs genistein (52%), daidzein (42%), and glycitein (6%), and the total content of soy phytoestrogens in SoyAct was about 30%. The remaining 70% of the extract used in the present study was reported to contain saponin, protein, sugar, fat, moisture, ash, and fiber (Yamakoshi *et al.*, 2000). The protein component of the extract was composed of amino acids and peptides, which had molecular weights < 10,000 Da. The extract did not contain vitamin E.

***Animals.*** A total of 68 female 4-week-old Donryu rats (Japan SLC, Shizuoka, Japan) were quarantined for 1 week before the start of the experiment. They were housed in an animal facility maintained on a 12-h (7:00–19:00) light/dark cycle, at a constant temperature of 23 ± 1°C and relative humidity of 44 ± 5%, and were given free access to tap water and NIH-07PLD diet (phytoestrogen-low diet; Oriental Yeast, Tokyo, Japan). NIH-07PLD diet contained crude protein, carbohydrate, fat, crude fiber, neutral detergent fiber, ash, amino acids, fatty acids, vitamins, and trace elements with no phytoestrogens. All experimental procedures were conducted following approval of the Animal Care and Use Committee of the Osaka City University Medical School. Guidelines set by the National Institute of Health and Public Health Service Policy on the Humane Use and Care of Laboratory Animals were followed at all times.

***Experiment 1.*** Ten 5-week-old female Donryu rats with normal estrous cycles were selected, and ovariectomy was performed. Absence of estrous cycles after the operation was confirmed with vaginal smears. Two weeks after the operation, rats were given 0.6% IA-rich extract (0.2% IA) in basal NIH-07PLD diet or only control diet only for a further 2 weeks. In this case, a rat (body weight 200 g) consumes IA in 15 g diet at a dose of 150 mg/kg body weight/day (100 times of ADI for human [the accepted by WHO safety factor in terms of ADI for rats is 100]), which is equal to about 1.5 mg/kg body weight/day intake by women with mean body weight 50 kg (ADI for human is 75 mg/day) (Lu, 1988). Alternatively, the animal dose could be extrapolated to a human equivalent dose by using the body surface area normalization method (mg/m$^2$ conversion) (Freireich *et al.*, 1966; Reagan-Shaw *et al.*, 2008). In such conversion, extrapolating from human to rat involves multiplying the human dose by 6.16 (Km human/Km animal = 37/6). If using this extrapolation, the animal dose 150 mg/kg body weight/day used in the present study will be equal to about 24 mg/kg body weight/day intake by human.

All animals were checked for general condition at least once a day. Body weights were measured once a week. At sacrifice, uterine weights were measured to detect estrogenic activity of 0.2% IA. Furthermore, histological examination of the uterus, mammary gland, liver, kidneys, spleen, adrenals, and thymus was performed.

***Experiment 2.*** Five 5-week-old female rats received 50 mg/kg DMBA in sesame oil/kg body weight (ig), and another five were given an equivalent volume of sesame oil (~0.5 ml/rat, ig). Rats were administered IA-rich extract at a dose of 0.6% (0.2% IA) in NIH-07PLD diet or basal diet only for 4 weeks starting from the day of DMBA injection. Animals were killed by deep anesthesia with diethyl ether, and skin and mammary gland samples were obtained and fixed in 10% phosphate-buffered formalin. Representative sections of each mammary gland were routinely processed for pathological examination and bromodeoxyuridine (BrdU) immunohistochemistry. In addition, uterus, liver, kidneys, spleen, adrenals, thymus, and weights were measured.

***Experiment 3.*** At 5 weeks of age, 48 female Donryu rats were selected and divided into three groups. Donryu rats' pubertal development starts soon after weaning, from about postnatal day 35. Rats were inspected daily for vaginal opening since onset of puberty is defined as the age (in days) at which vaginal opening occurred. To initiate mammary carcinogenesis, 5-week-old rats in IA-treated and initiation control groups (21 rats per group) were given a single dose of DMBA by ig (50 mg/kg body weight) at the commencement of the experiment. ENNG (10 mg/kg body weight) in PEG was administered via the vagina using a stainless catheter on experimental days 7 and 11 to initiate uterine carcinogenesis. In the control group, six animals received sesame oil by ig and PEG via the vagina as the vehicle. Animals were administered the IA-rich extract at a dose of 0.6% (0.2% IA) in NIH-07PLD basal diet or control basal diet for 40 weeks starting from the commencement of the experiment. All animals were checked for general condition at least once a day. Body weights were measured once a week. The estrous cycle status was ascertained at 3-month intervals with vaginal smears throughout the study. Age-related persistent estrus followed by anovulation in Donryu rats was reported to be started at 5 months of age, and its incidence was markedly increased until 8 months (Nagaoka *et al.*, 2000). Multiplicity and volume of mammary tumors were examined every week, and location of every nodule was recorded and diagnosed after final histopathological examination. Mammary gland tumor volume being calculated as tumor length/2 × (width/2)$^2$ and expressed as cm$^3$/rat. In contrast to benign tumors, malignant mammary tumors appeared dark and most of them developed metastasis to the lung. Furthermore, malignant tumors developed ulcers and abscesses, which were absent in benign tumors. Histopathological analysis was performed according to the classification of mammary tumors delineated previously by applying the histopathological criteria (Costa *et al.*, 2002; Young and Hallowes, 1973). Among these criteria, the most useful were the analyses of the loss or preservation of the tubuloalveolar pattern of the normal mammary gland, cell population,

Downloaded from http://toxsci.oxfordjournals.org/ at Oska City University - Medical Campus on February 28, 2012

cytological features, such as number of mitoses or nuclear enlargement and the presence or absence of invasion of the stroma and neighboring tissues.

Complete necropsies were done on all surviving animals at week 40 after the initiation with DMBA (45 weeks of age). The following organs were removed and weighed: uterus, skin with mammary glands, ovaries, liver, pituitary, and adrenals. The ovaries, uteri, vaginas, and other representative organs were fixed in 10% phosphate-buffered formalin solution and then routinely processed for histopathological examination. Animals found dead or killed when moribund were also autopsied and sampled for histopathology. Each uterus was dissected into about 12 specimens in cross-section, and proliferative endometrial lesions were classified into 3° of atypical hyperplasias, adenocarcinomas, stromal, and adenomatous polyps using the categories described in previous report (Nagaoka *et al.*, 1994).

***LC-MS/MS, iTRAQ labeling, and quantification of protein expression.*** Proteome analysis was performed on a DiNa-AI nano LC System (KYA Technologies, Tokyo, Japan) coupled to a QSTAR Elite hybrid mass spectrometer (AB Sciex, Concord, Canada) through a NanoSpray ion source (AB Sciex) as described previously (Kakehashi *et al.*, 2011). Each sample was run for 150 min.

Because of the difficulties of collection of normal mammary gland and uterine endometrium tissues by microdissection, it was decided to use the pooled samples for proteome analysis. The lysis buffer was chosen and adjusted specially to use with formalin-fixed and paraffin embedded (FFPE) sections according to the recently published method (Klein *et al.*, 2011). Furthermore, we have performed comparative analysis of frozen tissue and FFPE sections Liquid chromatography with tandem mass spectrometry (LC-MS/MS) of different animal tissues, which demonstrated high concordance of results. Duplicate pooled samples from microdissected and/or needle dissected 10% phosphate-buffered formalin-fixed mammary adenocarcinomas (DMBA, ENNG: 1 rat, DMBA, ENNG→0.2% IA: 6 rats), uterine adenocarcinomas and severe atypical hyperplasias (DMBA, ENNG: 3 rats, DMBA, ENNG→0.2% IA: 6 rats) and normal-appearing mammary gland (DMBA, ENNG: 20 rats, DMBA, ENNG→0.2% IA: 20 rats), or endometrium (DMBA, ENNG: 20 rats, DMBA, ENNG→0.2% IA: 20 rats) from rats in initiation control group and group administered 0.2% IA after the DMBA and ENNG treatment were prepared in 20mM Tris-HCl buffer, pH 8, with 0.002% Zwittergent, treated with heat at 90°C for 90 min (spin down every 20 min), digested with trypsin at 37°C for 16–18 h, and centrifuged at 12,350 × g for 1 min. Protein concentrations were measured with BCA Protein Assay Kit (Pierce, IL). Each pooled sample contained 10 μg protein. Thereafter, labeling was performed with 4-plex iTRAQ reagents according to standard procedures (Gluckmann *et al.*, 2007). Pooled samples were labeled as described below: iTRAQ isobaric reagents 114, normal mammary gland or endometrium in DMBA, ENNG→0.2% IA-treated groups; 115, mammary adenocarcinomas or uterine adenocarcinomas and severe atypical hyperplasias in DMBA, ENNG→0.2% IA-treated groups; 116, normal mammary gland or endometrium in DMBA, ENNG treated groups; and 117, mammary adenocarcinomas or uterine adenocarcinomas and severe atypical hyperplasias in DMBA, ENNG control groups. MS/MS data were searched against the Swiss Protein database (RAT) using ProteinPilot software (version 2.0; AB Sciex) with trypsin set as the digestion enzyme and methyl methanethiosulfonate as the cysteine modification. The search results were further processed by ProteinPilot software using the Paragon Algorithm for redundant hits removing and comparative quantitation, resulting in the minimal set of justifiable identified proteins. Each sample was measured three times, and all reported data were used at 95% confidence cutoff limit created by ProteinPilot software. The same program was used to remove the bias for proteins expressed at very low levels. Protein ratios with a $p$ value less than 0.05 were considered reliable. Previously, SDs of the protein ratio, which stem from technical variation, were reported to be less than 0.3 in 90% of iTRAQ experimental runs (Song *et al.*, 2008). In this experiment, expression changes greater than 1.3-fold or less than 0.769-fold in normalized expression levels were decided to be outside the range of technical variability.

***Ingenuity Pathway and Bioinformatic analyses.*** To assign biological significance to differentially labeled proteins, to identify networks of interacting proteins, functional groups, and pathways, and to determine whether the protein candidates were known plasma proteins, secreted or membrane proteins or were associated mammary gland or uterus, cancer, the Ingenuity program (Ingenuity Systems, Mountain View, CA) was utilized. Proteins known to be associated with cancer biology were prioritized for further validation. Bioinformatic analysis of gene promoters encoding proteins with altered expression was performed using PROMOSER and TFSEARCH Internet databases for identification of common transcriptional factors that may be driving the expression changes.

***Immunohistochemical examination.*** For the evaluation of cellular proliferation in the rat uterus and mammary glands, BrdU (experiment 1) and PCNA (experiment 2) immunohistochemistry were performed as previously described (Kinoshita *et al.*, 2003). In experiments 1 and 2, all 12 specimens in cross-section of uterus from all rats were subjected to the analysis. BrdU and PCNA indices were assessed as the number of positive nuclei per 1000 cells.

Paraffin sections containing preneoplastic and neoplastic lesions as well as normal mammary gland and uterus tissues were used for comparison and stained using standard immunohistochemical methods. Goat polyclonal antibodies against annexin 1, kininogen 1 and cadherin, EGF LAG seven-pass G-type receptor 2 (Santa Cruz Biotechnology Inc.), rabbit polyclonal antibodies against annexin 2, DEAD box polypeptide 1, destrin, cysteine- and glycine-rich protein 1 and S100 calcium-binding protein A8 (Abcam Co., Japan), ER-alpha (ER-α) (Santa Cruz Biotechnology Inc.), and ER-beta (ER-β) (Millipore, Upstate) were employed for immunohistochemical validation of the results of the proteome analysis in the mammary gland and uterus (Supplementary data). Immunohistochemical procedures were optimized by testing different antigen retrieval methods and negative controls.

***Statistical analysis.*** Statistical analysis was performed using the StatLight-2000(C) program (Yukms Corp., Japan) or the IBM SPSS Statistics 19 Software (IBM). Fisher's exact probability test or the $\chi^2$-test and log-rank test were used to compare the tumor incidence of histopathological lesions. Homogeneity of variance was tested by the $F$-test. Differences in mean values for tumor multiplicities and volumes between the initiation control and the IA-treated groups were evaluated by the two-tailed Student's $t$-test when variance was homogeneous and the two-tailed Aspin-Welch $t$-test when variance was heterogeneous. Survival curves were calculated using the Kaplan-Meier method, and differences in survival curves were assessed with the log-rank test. $p$ values less than 0.05 were considered significant. For analysis of protein expression, ProteinPilot 2.0 Software was employed.

## RESULTS

### *Short-Term Studies (Experiments 1 and 2)*

*Estrogenic effect of 0.2% IA.* After ovariectomy in experiment 1, 0.2% IA administration resulted in persistent estrus evident on examination of vaginal smears (data not shown). Mean relative uterus weight was significantly elevated in 0.2% IA-administered ovariectomized rats (0.58 ± 0.13%, $p < 0.005$) as compared with control rats (0.32 ± 0.04%), thus demonstrating estrogenic activity of the 150 mg/kg body weight/day dose of IA in the rat uterus (data not shown). After confirmation of the estrogenic effect of 0.2% IA, this dose was applied in experiments 2 and 3 to study the modifying effects of a hormonal dose of IA on rat endometrial and mammary carcinogenesis. In short-term experiments, no changes in body weight were observed in IA-treated rats as compared with the initiation control groups.

Downloaded from http://toxsci.oxfordjournals.org/ at Oska City University - Medical Campus on February 28, 2012

*Alteration of cell proliferation.* In experiment 1, PCNA-positive cell indices were strongly elevated in the uterus endometrium (309.48 ± 55.30 $PCNA^+$ cells/1000 cells, $p < 0.0001$) of ovariectomized rats treated for 2 weeks with 0.2% IA as compared with the control group (27.39 ± 7.63 $PCNA^+$ cells/1000 cells) (data not shown). Furthermore, in experiment 2, BrdU immunohistochemistry revealed a significant increase of number of positively stained cells in the terminal end buds of the mammary gland (33.20 ± 4.17 $BrdU^+$ cells/1000 cells, $p < 0.001$) and a trend for increase in the uterine endometrium (145.02 ± 104.55 $BrdU^+$ cells/1000 cells) after 4 weeks administration of 0.2% IA as compared with controls (mammary gland: 17.13 ± 2.27 $BrdU^+$ cells/1000 cells and uterus: 115.39 ± 103.19 $BrdU^+$ cells/1000 cells).

*Long-term Study (Experiment 3)*

*General observations.* Four animals in the initiation control group and six animals in 0.2% IA-administered group died during the study. The causes in the initiation control group were malignant lymphoma/leukemia (three rats) and zymbal gland tumor (one rat). No animals died from uterine or mammary gland cancers. On the other hand, in the 0.2% IA-treated group, causes of death were mammary adenocarcinomas (three rats), uterine adenocarcinoma (one rat), and bleeding from large necrotic mammary tumors (two rats). Three IA-treated rats featured metastasis of mammary adenocarcinomas in the lung. Significant increase of mammary tumor volumes measured macroscopically was observed in the group treated with IA compared with the initiation control group (from week 29 to week 32) (Fig. 1C). However, due to the sudden growth of benign tumors in the mammary gland of the initiation control group starting from week 32 up to the termination of the experiment, a significant decrease of total mammary tumor volume was finally observed in the IA-treated rats.

The body weights of 0.2% IA-treated rats were significantly depressed starting from the first week ($p < 0.05$) of IA application up to the termination of the experiment at week 40 ($p < 0.0001$) compared with the initiation control group (Fig. 1D). Body weights of IA-treated animals demonstrated 10% reduction from week 10 to 20, 16% reduction at week 30, and 19% reduction at the termination at week 40. Food intake did not differ between groups. However, water intake was significantly depressed by IA application, starting from the first week and up to week 40.

No significant differences in uterus, liver, kidneys, spleen, heart, thymus pituitary, and adrenals weights were observed (data not shown).

*Survival curves (experiment 3).* At week 15, the first rat from the initiation control group was found dead with a lymphoma/leukemia. The number of surviving IA-administered animals started quickly to decrease at week 21, mostly due to the development of mammary and uterine tumors, which were not found in the initiation control group (Fig. 1E). A trend for decrease in survival rate of IA-treated rats, however, without significant difference compared with the initiation control group, was found at final sacrifice.

*Histopathological findings in the mammary gland.* The results for macroscopically evident mammary gland tumor incidences, multiplicities and volumes, as well as histopathological analysis and representative pictures are presented in Table 1 and Figures 1A–C and 2A (a–d). In the group administered 0.2% IA, significant increases of mammary gland adenocarcinoma incidence (week 33–36) and multiplicity (week 32–36) as compared with the initiation control rats were observed (Figs. 1A and 1B). The onset of tumor development in rats administered IA (adenocarcinomas: week 15) was earlier than that of initiation control rats (benign tumor: week 19) (Figs. 1A and 1B). Unexpectedly, due to the sudden development of benign tumors in the mammary gland of the DMBA, ENNG control group starting from week 32, a significant decrease of total benign tumor incidence and multiplicity was finally detected in the IA-treated group (Figs. 1A and 1B).

Histopathological analysis of the mammary gland tumors at termination of the experiment demonstrated significant elevation of adenocarcinoma incidence ($p < 0.05$) and multiplicity ($p < 0.05$) in IA-administered rats. On the other hand, significant decrease of fibroadenoma ($p < 0.05$) and total tumors multiplicities in the group fed IA after initiation was found (Table 1). Furthermore, a trend for decrease was detected for the incidence of benign tumors in the group of animals treated with IA (Table 1).

*Histopathological findings in the uterus.* The results of histopathological analysis of rat uteri are presented in Table 1 and Figure 2A (e–l). At necropsy, the uteri in IA-treated rats demonstrated increased hemorrhage, dilatation, and higher numbers of nodules macroscopically (data not shown). Histopathologically, most of the animals in the initiation control and IA-treated groups demonstrated various proliferative lesions in the uteri, with a sequence of changes from atypical hyperplasias to adenocarcinomas (Fig. 2A [e–h]) as well as development of stromal and adenomatous polyps (Fig. 2A [i–l]). A significant increase in the multiplicities of total atypical hyperplasia (HPL) (mild, medium, and severe) and total endometrial proliferative lesions (adenocarcinoma + atypical HPL) was found in the uteri of IA-administered animals (Table 1). A trend for increase was also observed for the incidence and multiplicity of endometrial adenocarcinomas in the IA-treated group as compared with the initiation control rats. Moreover, a significant elevation of multiplicities of adenomatous polyps was detected in the uteri of the IA-administered group (Table 1 and Fig. 2A [i–l]).

*Alterations of protein expression in mammary adenocarcinomas.* The results of the QSTAR Elite LC-MS/MS and Ingenuity Pathway analyses (IPA) of the mammary gland

Downloaded from http://toxsci.oxfordjournals.org/ at Oska City University - Medical Campus on February 28, 2012

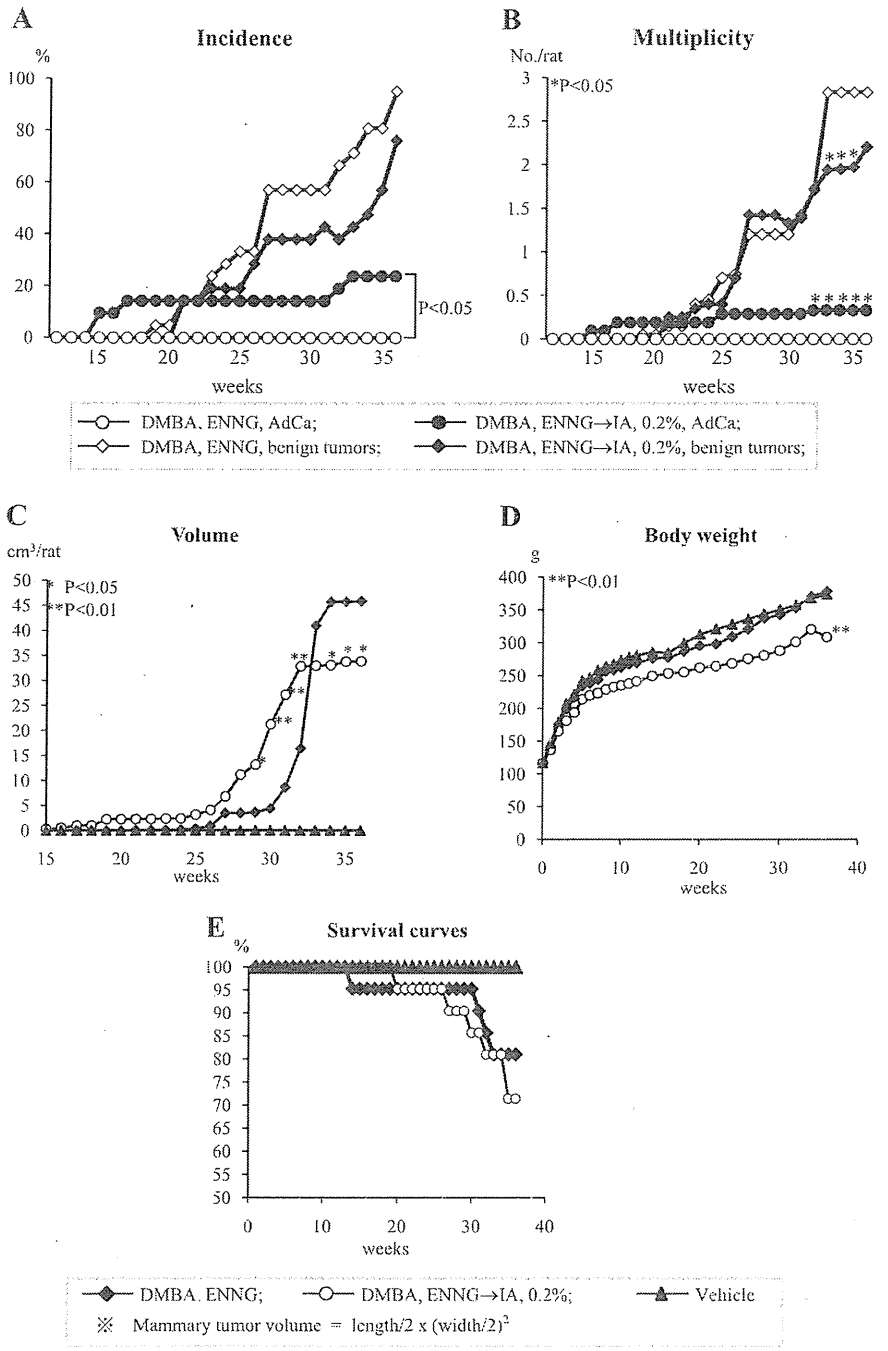


**FIG. 1.** (A) Incidence and (B) multiplicity of mammary tumors in female Donryu rats in experiment 3, (C) volume of mammary tumors examined every week during the experiment, (D) body weights, and (E) survival curves of Donryu rats. Significant increase of mammary adenocarcinoma incidence and multiplicity in DMBA, ENNG→0.2% IA-administered rats, and on the other hand, decrease of benign tumors multiplicity was found. Furthermore, early elevation of mammary adenocarcinomas incidence, multiplicity, and tumors volume in IA-administered rats was observed from week 15.

adenocarcinomas compared with the normal-appearing mammary gland tissue of rats from initiation control and IA-treated animals are presented in Table 2.

Interestingly, only in the adenocarcinomas of IA-treated animals, significant overexpression of S100 calcium-binding protein A8 (S100A8) (12.38-fold), involved in cell cycle progression and angiogenesis, as well as kininogen 1 (KNG1) (5.1-fold), which is an F-actin–associated protein participating in phosphorylation and activation of epidermal growth factor receptor (EGFR), was found (Table 2). Furthermore, as

Downloaded from http://toxsci.oxfordjournals.org/ at Oska City University - Medical Campus on February 28, 2012

TABLE 1
Incidence and Multiplicity of Neoplastic Lesions in the Mammary Glands and Uterus of Donryu Rats

| Treatment / Mammary gland | Number of rats[a] | Fibroadenoma | Fibroma | Adenoma | AdCa | Total |
|---|---|---|---|---|---|---|
| Incidence (number of rats (%)) | | | | | | |
| DMBA, ENNG | 21 | 20 (95.4) | 7 (33.3) | 3 (14.3) | 1 (4.8) | 20 (95.2) |
| DMBA, ENNG→IA, 0.2% | 21 | 18 (85.7) | 3 (14.3) | 2 (9.5) | 6 (28.6)[b] | 21 (100) |
| Vehicle | 5 | 1 (20) | 0 | 0 | 0 | 1 (20) |
| Multiplicity (number/rat) | | | | | | |
| DMBA, ENNG | 21 | 10.38 ± 4.93 | 0.52 ± 0.87 | 0.14 ± 0.36 | 0.05 ± 0.22 | 11.10 ± 5.35 |
| DMBA, ENNG→IA, 0.2% | 21 | 6.90 ± 5.02[b] | 0.14 ± 0.36 | 0.10 ± 0.30 | 0.43 ± 0.75[b] | 7.57 ± 4.87[b] |
| Vehicle | 5 | 0.20 ± 0.45 | 0 | 0 | 0 | 0.20 ± 0.45 |

| | | Endometrial HPL | | | | | | Polyps | |
|---|---|---|---|---|---|---|---|---|---|
| Uterus | | Mild | Moderate | Severe | Total | AdCa | AdCa + HPL | S | A |
| Incidence (number of rats (%)) | | | | | | | | | |
| DMBA, ENNG | 21 | 10 (47.6) | 5 (24) | 2 (9.5) | 17 (81.0) | 1 (4.8) | 17 (81.0) | 6 (28.6) | 3 (14.3) |
| DMBA, ENNG→IA, 0.2% | 21 | 16 (76.2) | 5 (24) | 4 (19.0) | 20 (95.2) | 2 (9.5) | 20 (95.2) | 9 (42.9) | 9 (42.9) |
| Vehicle | 5 | 0 | 0 | 0 | 0 | 0 | 0 | 0 | 0 |
| Multiplicity (number/rat) | | | | | | | | | |
| DMBA, ENNG | 21 | 0.7 ± 0.8 | 0.2 ± 0.4 | 0.1 ± 0.5 | 1.1 ± 0.7 | 0.05 ± 0.22 | 1.01 ± 0.70 | 0.3 ± 0.6 | 0.1 ± 0.4 |
| DMBA, ENNG→IA, 0.2% | 21 | 1.1 ± 0.7 | 0.2 ± 0.4 | 0.2 ± 0.4 | 1.5 ± 0.6[b] | 0.10 ± 0.30 | 1.52 ± 0.60[b] | 0.6 ± 0.8 | 0.6 ± 0.8[b] |
| Vehicle | 5 | 0 | 0 | 0 | 0 | 0 | 0 | 0 | 0 |

*Note.* Values are mean ± SD. AdCa, adenocarcinoma; HPL, hyperplasia; AdCa + HPL, summarized data for adenocarcinoma and total hyperplasia; S, stromal polyp; A, adenomatous polyp.

[a]Effective number of rats.

[b]Significantly different from the DMBA, ENNG control group at $p < 0.05$.

compared with the protein spectrum of initiation control rats, in adenocarcinomas of IA-administered group, an elevation of expression was observed for proteins participating in cellular assembly and organization pathways, including annexin 1 (ANXA1), annexin 2 (ANXA2) and cytokeratin 8 (CK8) (fusion of liposome, aggregation of cellular membrane, organization of filaments), cytokeratin 5 (CK5), capping protein (actin) muscle Z-line, alpha 2 (CAPZA2) and transgelin (TAGLN) (organization of F-actin), fibronectin (FN1), tubulin beta 2C (TUBB2C), LMNA (detachment of desmin filament, morphology of nucleus), and thymopoietin (TMPO) (assembly of inner nuclear membrane). Moreover, elevated expression of cellular chaperone heat shock–related endoplasmic reticulum protein 29 (ERP29) involved in NRF2-mediated oxidative stress response, poly(A)-binding protein cytoplasmic 1 (PABPC1) promoting ribosome recruitment and translation initiation was detected. In addition, in IA-treated rats, significant downregulation of decorin (DCN), an anti-tumorigenic protein capable of suppressing the growth of various tumor cell lines and interaction with EGFR and TGF-β, was obvious (Table 2).

Proteome analysis of the normal mammary gland tissue of rats treated with IA when compared with the normal mammary gland of initiated control rats demonstrated upregulation of CK8, PDIA3, and HSP90AB1 and downregulation of DCN, similar to that observed in adenocarcinomas of IA-administered animals, which might be indicative of occurred cellular stress and activation of ER signaling.

*Alteration of protein expression in endometrial proliferative lesions.* Data from proteome and IPA of the uterine proliferative lesions compared with protein expression of the normal endometrium of rats 40 weeks after initiation or after treatment with IA are presented in Table 2.

As compared with the protein spectrum of the initiation control rats endometrial proliferative lesions, in IA-administered animals, a significant increase of flamingo cadherin, EGF LAG seven-pass G-type receptor 2 (CELSR2), a receptor involved in contact-mediated communication with cadherin and EGF-like domains, cysteine- and glycine-rich protein 1 (CSRP1) and destrin (DSTN), two proteins participating in Rho-dependent organization of F-actin, RNA helicase DEAD box polypeptide 1 (DDX1), and downregulation of decorin, as in mammary adenocarcinomas, was found (Table 2).

In the normal endometrium of IA-administered rats, upregulation of CK8, 19, TAGLN, histones HIST2H2AA3, HIST1H2BH, HIST1H1D, and desmin (DES) and downregulation of DCN as compared with the normal-appearing endometrium of rats in initiation control group were detected (data not shown).

Downloaded from http://toxsci.oxfordjournals.org/ at Oska City University - Medical Campus on February 28, 2012

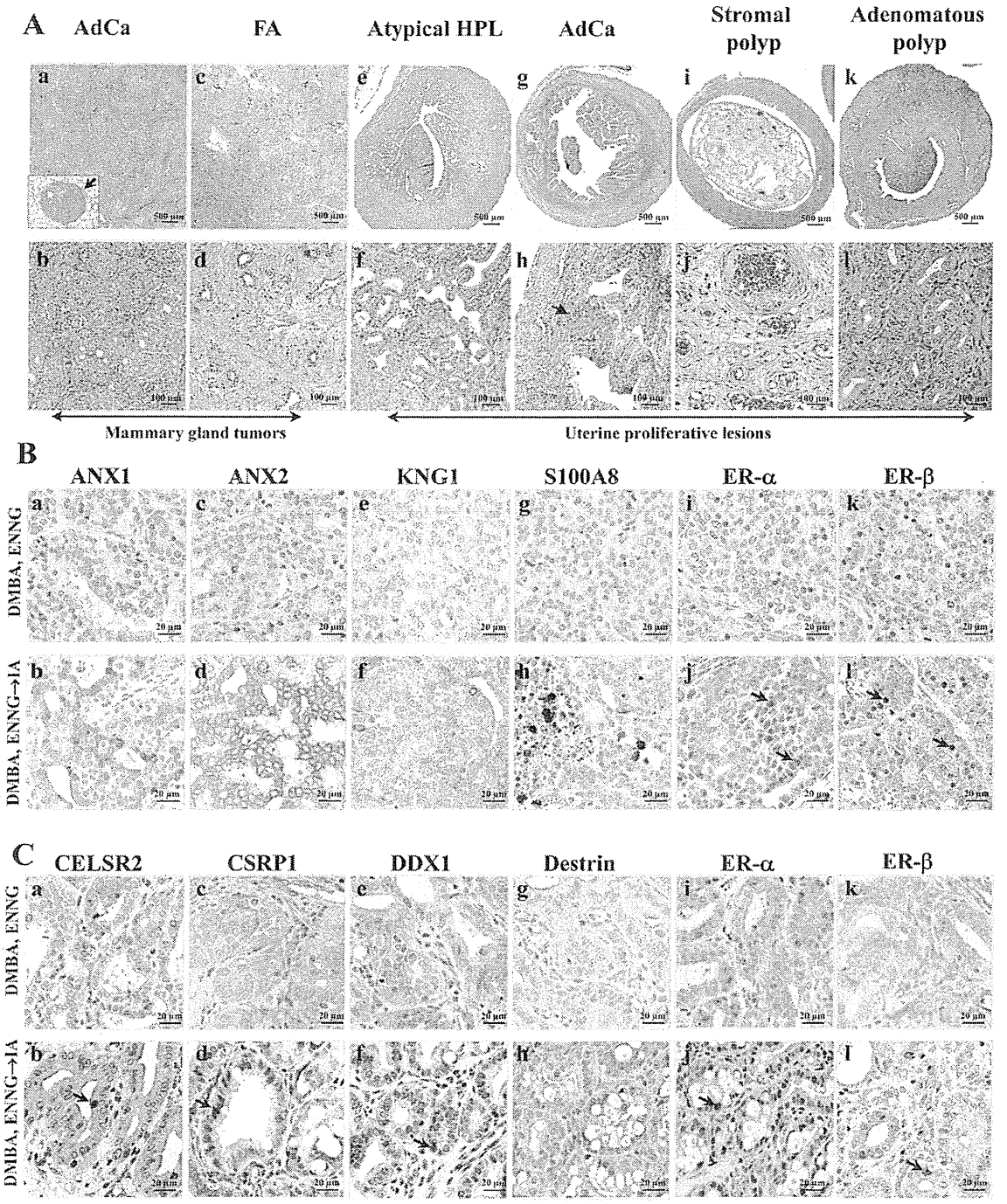


**FIG. 2.** (A) Representative histopathological changes in the mammary gland (a–d) and uteri (e–l) observed in both initiation control and IA-treated animals (hematoxylin and eosin). Moderate atypical hyperplasia is composed of an increased number of glands under the lining epithelium (e and f). Well-differentiated endometrial adenocarcinoma (AdCa) (g and h). Atypical glands in the endometrium are irregularly proliferating and invading the muscle layer (arrow). Stromal polyp (i and g) and adenomatous polyp (k and l) (magnification ×20 [a, c, e, g, i, and k) and ×200 (b, d, f, h, j, and l]). (B) Immunohistochemistry for ANX1 (a and b), ANX2 (c and d), KNG1 (e and f), S100A8 (g and h), ER-α (i and j), and ER-β (k and l) in the mammary gland and (C) immunohistochemistry for CELSR2 (a and b), CSRP1 (c and d), DDX1 (e and f), destrin (g and h), ER-α (i and j), and ER-β (k and l) in uterine adenocarcinoma and severe hyperplasia of initiation control (a, c, e, g, i, and k) and IA-administered rats (b, d, f, h, j, and l) (magnification ×400). Note increased nuclear expression of ER-α and ER-β in both mammary adenocarcinomas and uterine proliferative lesions of rats treated with IA. Significant cytoplasmic and membranous overexpression of ANX1 and particularly ANX2, cytoplasmic elevation of KNG1, and an increase of S100A8 in inflammatory cells were observed in the mammary AdCa of IA-treated animals. Furthermore, nuclear elevation of CELSR2, CSRP1, and DDX1 (arrows) and cytoplasmic overexpression of destrin were evident in uterine proliferative lesions of rats administered IA.

Downloaded from http://toxsci.oxfordjournals.org/ at Oska City University - Medical Campus on February 28, 2012

TABLE 2
**Differentially Expressed Proteins in Mammary Gland Adenocarcinomas and Uterine Proliferative Lesions of Donryu Rats at Week 40**

| Tissue/protein | GI number | Location | Type | Function | DMBA, ENNG | | DMBA, ENNG→0.2% IA | |
|---|---|---|---|---|---|---|---|---|
| | | | | | FC | *p* | FC | *p* |
| Mammary gland adenocarcinomas | | | | | | | | |
| Annexin A1 (ANXA1) | 113947 | PM | O | ST | 2.30 | 0.0100 | 3.73 | 0.0006 |
| Annexin A2 (ANXA2) | 584760 | PM | O | ST | — | — | 1.72 | 0.004 |
| Cytokeratin 8 (CK8) | 1708592 | C | O | CS | 4.41 | 0.0000 | 6.52 | 0.0000 |
| Cytokeratin 19 (CK19) | 73920214 | C | O | CS | 4.12 | 0.0068 | 4.12 | 0.0032 |
| Cytokeratin 5 (CK5) | 81170669 | C | O | CS | — | — | 3.65 | 0.0009 |
| Ezrin (EZR) | 68067388 | C | O | CS | 4.08 | 0.0008 | 2.71 | 0.0453 |
| WD repeat domain 1 (WDR1) | 81910041 | ES | O | CS | 1.70 | 0.0429 | 1.98 | 0.0366 |
| Myosin, heavy chain 9, nonmuscle (MYH9) | 13431671 | C | E | CS | 1.23 | 0.0032 | 1.64 | 0.0015 |
| Kininogen 1 (KNG1) | 125508 | ES | O | CS | — | — | 5.10 | 0.0186 |
| Capping protein (actin) muscle Z-line, alpha 2 (CAPZA2) | 1345696 | C | O | CS | — | — | 1.84 | 0.0087 |
| Transgelin (TAGLN) | 401095 | C | O | CS | — | — | 2.74 | 0.0446 |
| Fibronectin 1 (FN1) | 120178 | PM | E | CS | — | — | 2.39 | 0.0218 |
| Tubulin, beta 2C (TUBB2C) | 81892373 | C | O | CS | — | — | 2.39 | 0.0057 |
| Heat shock 70-kDa protein 5 (HSPA5) | 121574 | C | O | PF | 2.20 | 0.0000 | 2.49 | 0.0000 |
| Heat shock protein 90-kDa alpha, B1 (HSP90AB1) | 122065211 | C | O | PF | 2.60 | 0.0000 | 2.77 | 0.0000 |
| Protein disulfide isomerase family A, member 3 (PDIA3) | 1352384 | C | E | PF | 1.71 | 0.0005 | 1.95 | 0.0000 |
| Endoplasmic reticulum protein 29 (ERP29) | 2507015 | C | T | PF | — | — | 1.71 | 0.0252 |
| Histone H2A type 2A (HIST2H2AA3) | 74757558 | N | O | TR | 1.79 | 0.0001 | 1.93 | 0.0000 |
| Histone H2B type 1 (HIST1H2BH) | 399856 | N | O | TR | 3.38 | 0.0000 | 1.97 | 0.0000 |
| Histone H1D (HIST1H1D) | 1170152 | N | O | TR | 2.55 | 0.0000 | 1.68 | 0.0000 |
| Heterogeneous nuclear ribonucleoprotein M (HNRNPM) | 71152132 | PM | TMR | TR | 3.36 | 0.0274 | 2.57 | 0.0008 |
| Enolase 1, (alpha) (ENO1) | 56757324 | C | E | TR | 3.02 | 0.0001 | 3.59 | 0.0000 |
| HLA-B–associated transcript 1 (BAT1) | 61217662 | N | E | TR | 1.95 | 0.0061 | 1.72 | 0.0219 |
| Lamin A/C (LMNA) | 1346413 | N | O | NEO | — | — | 1.39 | 0.0055 |
| Thymopoietin (TMPO) | 46576200 | N | O | NEO | — | — | 1.83 | 0.0099 |
| ATP synthase, H + tr., mit. F1 compl., α subunit 1, (ATP5A1) | 83300587 | C | T | OP, T | 1.68 | 0.0251 | 2.30 | 0.0001 |
| ATP synthase, H+ tr., mit. F1 compl., β polypeptide (ATP5B) | 114562 | C | T | OP, T | 1.70 | 0.0038 | 2.55 | 0.009 |
| Aldolase A, fructose-bisphosphate (ALDOA) | 113609 | C | E | M | 4.33 | 0.0318 | — | — |
| Fatty acid synthase (FASN) | 2506136 | C | E | M | 3.32 | 0.0003 | 2.24 | 0.0389 |
| Glyceraldehyde-3-phosphate dehydrogenase (GAPDH) | 122065190 | C | E | M | 1.75 | 0.0256 | 2.25 | 0.0017 |
| Poly(A)-binding protein, cytoplasmic 1 (PABPC1) | 47605941 | C | TRL | TRL | — | — | 2.07 | 0.0277 |
| Ribosomal protein SA pseudogene (Lamr1) | 730681 | PM | TMR | TRL | 2.24 | 0.0302 | — | — |
| S100 calcium-binding protein A8 (S100A8) | 13638435 | C | O | CC | — | — | 12.38 | 0.0440 |
| Valosin-containing protein (VCP) | 1174637 | C | E | VT | 2.66 | 0.0222 | 2.83 | 0.0432 |
| Olfactomedin-like 3 (OLFML3) | 221272402 | ES | O | U | — | — | 0.13 | 0.0480 |
| Decorin (DCN) | 266763 | ES | O | EMO | — | — | 0.16 | 0.0420 |
| Beta-casein (CSN2) | 5915877 | ES | T | T | 0.16 | 0.0091 | — | — |
| Uterine adenocarcinoma and severe hyperplasia | | | | | | | | |
| Annexin A1 (ANXA1) | 113947 | PM | O | ST | 1.56 | 0.0000 | 1.47 | 0.0088 |
| Annexin A5 (ANXA5) | 4033508 | PM | O | ST | 1.25 | 0.0127 | 1.39 | 0.0225 |
| Annexin A6 (ANXA6) | 1351943 | PM | O | ST | 1.52 | 0.0003 | 1.39 | 0.0342 |

Downloaded from http://toxsci.oxfordjournals.org/ at Oska City University - Medical Campus on February 28, 2012

TABLE 2—*Continued*

| Tissue/protein | GI number | Location | Type | Function | DMBA, ENNG | | DMBA, ENNG→0.2% IA | |
|---|---|---|---|---|---|---|---|---|
| | | | | | FC | *p* | FC | *p* |
| Cadherin, EGF LAG seven-pass G-type receptor 2 (CELSR2) | 22095545 | PM | G | ST | — | — | 1.47 | 0.0280 |
| Cytokeratin 8 (CK8) | 1708592 | C | O | CS | 2.47 | 0.0000 | 2.67 | 0.0000 |
| Cytokeratin 19 (CK19) | 73920214 | C | O | CS | 1.91 | 0.0012 | 1.49 | 0.0004 |
| Desmin (DES) | 1352241 | C | O | CS | 1.91 | 0.0000 | 1.70 | 0.0000 |
| Actinin, alpha 1 (ACTN1) | 13123942 | C | O | CS | 2.14 | 0.0014 | 2.33 | 0.0011 |
| Ezrin (EZR) | 68067388 | C | O | CS | 1.49 | 0.0038 | 1.55 | 0.0272 |
| Transgelin (TAGLN) | 401095 | C | O | CS | 1.85 | 0.0000 | 1.40 | 0.0000 |
| Capping protein (actin) muscle Z-line, alpha 2 (CAPZA2) | 1345696 | C | O | CS | 2.20 | 0.0417 | 2.20 | 0.0450 |
| Calponin 1, basic, smooth muscle (CNN1) | 584953 | C | O | CS | 1.81 | 0.0000 | 1.77 | 0.0000 |
| Tubulin, beta 2C (TUBB2C) | 81892373 | C | O | CS | 1.28 | 0.0043 | 1.49 | 0.0000 |
| Destrin (actin depolymerizing factor) (DSTN) | 126302540 | C | O | CS | — | — | 1.82 | 0.0023 |
| Histone H2A type 2A (HIST2H2AA3) | 74757558 | N | O | TR | 1.94 | 0.0125 | 1.91 | 0.0002 |
| Histone H2B type 1 (HIST1H2BH) | 399856 | N | O | TR | 1.58 | 0.0000 | 1.69 | 0.0000 |
| Histone H1D (HIST1H1D) | 1170152 | N | O | TR | 1.29 | 0.0000 | 1.34 | 0.0000 |
| Enolase 1, (alpha) (ENO1) | 56757324 | C | E | TR | 1.28 | 0.0118 | 1.46 | 0.0267 |
| DEAD (Asp-Glu-Ala-Asp) box polypeptide 1 (DDX1) | 76364171 | N, C | E | TR | — | — | 1.99 | 0.0497 |
| Poly(A)-binding protein, cytoplasmic 1 (PABPC1) | 47605941 | C | TRL | TRL | 1.75 | 0.0316 | 1.43 | 0.0336 |
| Polypyrimidine tract binding protein 1 (PTBP1) | 266862 | N | E | RP | 1.61 | 0.0070 | 1.37 | 0.0200 |
| Aldolase A, fructose-bisphosphate (ALDOA) | 113609 | C | E | M | 1.34 | 0.0016 | 1.46 | 0.0000 |
| Creatine kinase, brain (CKB) | 122065316 | C | K | M | 1.48 | 0.0041 | 1.45 | 0.0001 |
| Glyceraldehyde-3-phosphate dehydrogenase (GAPDH) | 122065190 | C | E | M | 1.56 | 0.0000 | 1.43 | 0.0000 |
| Heat shock 70-kDa protein 5 (HSPA5) | 121574 | C | O | PF | 1.49 | 0.0000 | 1.42 | 0.0193 |
| Heat shock 70-kDa protein 2 (HSPA2) | 148887381 | C | O | PF | 1.26 | 0.0319 | 1.24 | 0.0026 |
| Heat shock protein 90-kDa alpha, B1 (HSP90AB1) | 122065211 | C | O | PF | — | — | 1.37 | 0.0356 |
| Protein disulfide isomerase family A, member 3 (PDIA3) | 1352384 | C | E | PF | 1.49 | 0.0005 | 1 33 | 0.0001 |
| Lamin A/C (LMNA) | 1346413 | N | O | NEO | 1 67 | 0.0006 | 1.44 | 0.0007 |
| Cysteine- and glycine-rich protein 1 (CSRP1) | 1345932 | N | O | NSD | — | — | 1.52 | 0.0032 |
| Olfactomedin-like 3 (OLFML3) | 221272402 | ES | O | U | 0.66 | 0.0000 | 0.62 | 0.0084 |
| Decorin (DCN) | 266763 | ES | O | EMO | — | — | 0.62 | 0.0000 |

*Notes.* C, cytoplasm; N, nucleus; PM, plasma membrane; ES, extracellular space; CS, cytoskeleton; TR, transcriptional regulator; CC, cell cycle; E, enzyme; K, kinase; T, transporter; OP, oxidative phosphorylation; M, metabolism; TMR, transmembrane receptor; TRL, translation; NEO, nuclear envelope organization; PF, protein folding; EMO, extracellular matrix organization; G, G protein; VT, vesicle transport; RP, mRNA processing; SEC, secretion; DM, dendrite morphogenesis; NSD, nervous system development; U, unknown; O, other; —, no change of protein expression; FC, fold change as compared with normal-appearing tissue area.

*Orthogonal antibody–based validation.* To confirm proteome analysis results, we examined the protein expression in tumor tissue by immunohistochemistry. We focused our validation efforts on proteins for which antibodies with the prerequisite specificity were available. In the mammary gland adenocarcinomas, four proteins that met these criteria were ANXA1, ANXA2, KNG1, and S100A8, all of which were found to be overexpressed in 100% of mammary adenocarcinomas of IA-treated rats with low to undetectable expression in initiation control group (Fig. 2B [a–h]). In all adenocarcinomas of IA-administered animals, ANXA1 was present in tumor cells in a cytoplasmic distribution, whereas membranous or extracellular staining was observed for ANXA2 and KNG1. Strong positive staining for S100A8 was found in the inflammatory cells, in adenocarcinomas of IA-treated rats.

In 100% of uterine adenocarcinomas and 90% of atypical hyperplasias of the IA-administered group, CELSR2, CSRP1, and DDX1 were found in both nuclear and cytoplasmic compartments, whereas in all proliferative lesions of initiation

Downloaded from http://toxsci.oxfordjournals.org/ at Oska City University - Medical Campus on February 28, 2012

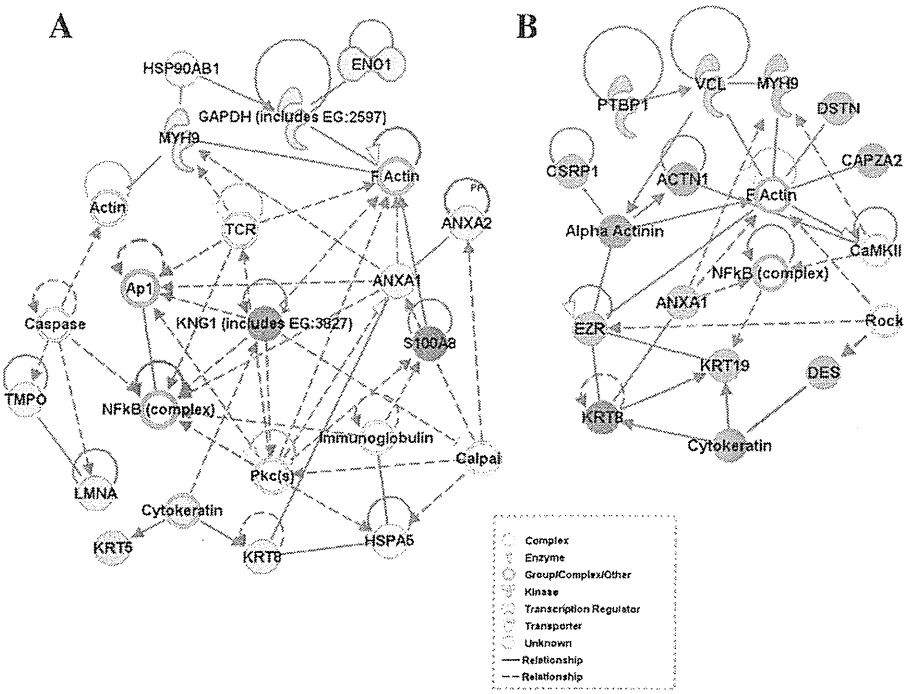


**FIG. 3.** Signaling pathways involving differentially expressed proteins in mammary gland adenocarcinomas (A) and uterine proliferative lesions (B) of rats treated with DMBA and ENNG and administered 0.2% IA controlled by AP1 and NF-κB transcriptional factors (compared initiation control and IA-treated groups). Note strong overexpression of KNG1 and S100A8 in mammary adenocarcinomas and various F-actin–associated proteins in the uterine proliferative lesions.

control animals CELSR2, CSRP1 expression was only cytoplasmic, and DDX1 nuclear expression was less prominent (Fig. 2C [a–h]). Furthermore, increased levels of DSTN in the cytoplasm were observed in all adenocarcinomas and 88% of atypical hyperplasias in the IA-treated group.

Additionally, to check the estrogenic response, we performed the immunohistochemical examination of ER-α and ER-β (Figs. 2B and 2C [i–l]). In all mammary and uterine adenocarcinomas and 91% of uterine atypical hyperplasias of IA-treated animals, predominant nuclear overexpression of ER-α and to lesser extent ER-β was detected. Furthermore, in proliferative lesions of rats in the IA group, a significant increase of ER-α and ER-β of cytoplasmic localization was found.

*Bioinformatic and IPA analyses.* Analyses of the promoter regions of genes encoding proteins with altered expression in mammary adenocarcinomas and uterine proliferative lesions of initiation and IA-treated groups demonstrated that common transcriptional factors, which may be driving the expression changes, are AP1 and nuclear factor-kappa B (NF-κB) (Figs. 3A and 3B; data not shown). Most of the differentially expressed proteins detected by QSTAR Elite MS/MS were targets for these transcriptional factors, containing binding sites and participated in reorganization of F-actin. Furthermore, IPA functional analysis indicated that in both mammary and endometrial adenocarcinomas of IA-administered rats, upregulated or downregulated proteins were related to cancer, reproductive and endocrine system disorders, cellular assembly and organization, cellular movement, inflammatory response, cellular growth and proliferation, DNA replication, recombination, and repair pathways (data not shown).

## DISCUSSION

The present study demonstrated that postpubertal exposure to IA-rich extract at a dose of 150 mg/kg body weight/day possessed estrogenic activity, induced cell proliferation in the mammary gland and endometrium, altered the molecular tumor environment, and promoted mammary and uterine carcinogenesis in Donryu rats induced by DMBA and ENNG. Furthermore, in IA-treated rats, the development of mammary adenocarcinomas metastasizing to the lung was observed, which were totally lacking in the initiation control rats. A decrease of body weight and adipose deposition in IA-treated rats observed in the present study was possibly due to antilipogenic effects described earlier in mice (Naaz *et al.*, 2003). Furthermore, this study demonstrated that starting from week 32, in the initiation control group, sudden development of mammary gland benign tumors but not adenocarcinomas

Downloaded from http://toxsci.oxfordjournals.org/ at Oska City University - Medical Campus on February 28, 2012

occurs. This fact might be of importance when analyzing the effects of IA treatments of different duration on mammary carcinogenesis in animal models.

Soy isoflavones are known to become distributed to a wide variety of tissues as IAs and conjugates, and the IA is thought to be a mixture of bioactive molecules (Gu *et al.*, 2005). Furthermore, IA was previously found to be absorbed in higher amounts than glycoside forms in humans (Izumi *et al.*, 2000), what might explain in part the detrimental effects observed in the present study. The timing of exposure to isoflavones is thought to be a critical component for an effect on breast cancer risk. Thus, it was reported that neonatal genistein treatment exerted its chemoprevention action by acting directly to enhance maturation of terminal ductal structures and by altering the endocrine system to reduce cell proliferation in the mammary gland (Lamartiniere *et al.*, 1995). In contrast, as detected in the present study, the postpubertal exposure of Donryu rats to hormonally active dose of IA increased cell proliferation and promoted mammary and uterine carcinogenesis in a two-step carcinogenesis model.

Utero and mammary trophic effects of IA were previously suggested to be due to potentiation of signaling via ER-α and ER-β (Messina and Wood, 2008), similar transactivation capacity in reporter gene transfected cells being observed with either receptor, the estrogen response element and a reporter gene (Messina and Wood, 2008). The effects of isoflavones, therefore, are thought to be dependent on the dose of exposure. "Physiological" concentrations are known as those achieved in the serum of persons consuming the commonly recommended daily dose of isoflavones of 50–100 mg (Wuttke *et al.*, 2007). In the majority of *in vitro* studies, in which MCF-7 cells derived from human mammary cancer were analyzed, physiological concentrations of soy extracts and pure isoflavones stimulated growth (Gutendorf and Westendorf, 2001; Harris *et al.*, 2005; Hsieh *et al.*, 1998; Wang *et al.*, 1996). Furthermore, in a human breast cancer cell line, hormonally active concentrations of soy isoflavones were shown to suppress the detoxification of reactive catechol metabolites of 17beta-estradiol (E2) and inhibit the activity of catechol-*O*-methyltransferase (COMT), an enzyme involved in the metabolic activation and inactivation of E2 that may lead to promotion of mammary carcinogenesis (Lehmann *et al.*, 2008).

In line with these results, we demonstrated that an estrogenic dose of an IA-rich extract manufactured as a soy isoflavone supplement with genistein as the main aglycone activated ER-α or ER-β and downstream AP1 and NF-κB transcriptional factors, furthermore potentiating F-actin signaling in mammary and uterine adenocarcinomas. Even in the normal-appearing mammary gland and endometrium, IA administration was associated with the induction of several cytoskeletal proteins, such as CK8, 19, and TAGLN, and the suppression of DCN expression, similar to that in adenocarcinomas, which might be related to activation of ER signaling. Previously, reorganization of F-actin regulated by Rho family proteins was shown to lead to the activation of a number of transcriptional factors, such as AP1 and NF-κB, with associated alteration of expression of various genes, and finally induction of proliferation, invasion, and metastasis by different cancers (Wang *et al.*, 2010). Furthermore, supporting our data, NF-κB activation was recently detected in endometrial carcinogenesis and was suggested to be a novel target of oncogenic KRAS (Mizumoto *et al.*, 2011).

To our knowledge, we present here the first evidence of conspicuous elevation of S100A8 and KNG1 and downregulation of DCN, an anti-tumorigenic protein capable of suppressing the growth of various tumor cell lines and interaction with EGFR and TGF-β, in mammary adenocarcinomas of IA-treated rats. The findings support the conclusion that IA at an estrogenic dose promotes invasiveness of mammary tumors. Activation of EGF receptor was previously reported to be an important factor for initiation and progression of malignancies, including breast cancers (Milanezi *et al.*, 2008).

Supporting our results, increase of calcium-binding protein S100A8, which promotes tubulin polymerization, phagocyte migration, infiltration of granulocytes and upregulates transcription of genes that are under the control of NF-κB, has been reported in human breast ductal carcinoma *in situ* (Carlsson *et al.*, 2005; Cross *et al.*, 2005; Seth *et al.*, 2003). Furthermore, detailed analysis of proximal promoter regions of human calprotectin, a heterodimer of S100A8 and S100A9, revealed common binding sites for distinct transcription factors, such as AP1, NF-κB, and C/EBP, suggesting a relation to S100A8 elevation observed in the present study (Gebhardt *et al.*, 2006).

KNG1 is known as an extracellular matrix F-actin–associated protein and inhibitor of thiol proteases participating in phosphorylation and activation of EGFR and from the present data might become a possible biomarker associated with promotion of mammary carcinogenesis and possibly invasiveness of mammary adenocarcinomas. Previously, its active peptide bradykinin, which increases phosphorylation of mouse Mapk1 protein involved in the mutant mouse *Egfr* gene in mouse Mef cells (Thomas *et al.*, 2006; Wunderer *et al.*, 1990), has been detected in malignant ovarian, colon, and breast carcinomas but not in benign tumors.

Induction of CELSR2, CSRP1, and DSTN, which participate in Rho-dependent organization of F-actin, as well as RNA helicase DDX1, was here observed in the endometrial adenocarcinomas of IA-administered rats, and downregulation of DCN might be suggested to be related to the promotion of endometrial carcinogenesis by a hormonally active dose of IA. Furthermore, the shift in CELSR2 and CSRP1 localization to the nuclei as well as increase of DDX1 nuclear expression might indicate their participation in ER-dependent signaling. Under normal conditions, the flamingo cadherins, such as CELSR2, specific functions of which have yet to be determined, are known to be located at the plasma membrane and act as receptors involved in contact-mediated communication,

Downloaded from http://toxsci.oxfordjournals.org/ at Oska City University - Medical Campus on February 28, 2012

with cadherin domains acting as homophilic binding regions and EGF-like domains involved in cell adhesion and receptor-ligand interactions (Nakayama *et al.*, 1998).

In conclusion, in the present study, long-term postpubertal treatment of Donryu rats with IA at a dose of 150 mg/kg body weight exerted promoting effects on mammary and uterine endometrial carcinogenesis after initiation with DMBA and ENNG. Furthermore, activation of ERs, AP1 and NF-κB, and F-actin signaling was apparent with the hormonally active dose of the IA-rich extract, associated with rise in ER-α and ER-β nuclear localization, which might have caused elevation of cell proliferation, leading to the promotion and progression to more malignant lesions.

## SUPPLEMENTARY DATA

Supplementary data are available online at http://toxsci.oxfordjournals.org/.

## FUNDING

Grant-in-Aid for Scientific Research from the Ministry of Health, Labor and Welfare of Japan.

## ACKNOWLEDGMENTS

We thank Masayo Inoue, Kaori Touma, and Rie Onodera for their technical assistance and Yukiko Iura for her help during preparation of this manuscript.

## REFERENCES

Banerjee, S., Li, Y., Wang, Z., and Sarkar, F. H. (2008). Multi-targeted therapy of cancer by genistein. *Cancer Lett.* **269,** 226–242.

Carlsson, H., Petersson, S., and Enerback, C. (2005). Cluster analysis of S100 gene expression and genes correlating to psoriasin (S100A7) expression at different stages of breast cancer development. *Int. J. Oncol.* **27,** 1473–1481.

Costa, I., Solanas, M., and Escrich, E. (2002). Histopathologic characterization of mammary neoplastic lesions induced with 7,12 dimethylbenz(alpha)anthracene in the rat: A comparative analysis with human breast tumors. *Arch. Pathol. Lab. Med.* **126,** 915–927.

Cross, S. S., Hamdy, F. C., Deloulme, J. C., and Rehman, I. (2005). Expression of S100 proteins in normal human tissues and common cancers using tissue microarrays: S100A6, S100A8, S100A9 and S100A11 are all overexpressed in common cancers. *Histopathology* **46,** 256–269.

Freireich, E. J., Gehan, E. A., Rall, D. P., Schmidt, L. H., and Skipper, H. E. (1966). Quantitative comparison of toxicity of anticancer agents in mouse, rat, hamster, dog, monkey, and man. *Cancer Chemother. Rep.* **50,** 219–244.

Gebhardt, C., Nemeth, J., Angel, P., and Hess, J. (2006). S100A8 and S100A9 in inflammation and cancer. *Biochem. Pharmacol.* **72,** 1622–1631.

Gluckmann, M., Fella, K., Waidelich, D., Merkel, D., Kruft, V., Kramer, P. J., Walter, Y., Hellmann, J., Karas, M., and Kroger, M. (2007). Prevalidation of potential protein biomarkers in toxicology using iTRAQ reagent technology. *Proteomics* **7,** 1564–1574.

Gu, L., Laly, M., Chang, H. C., Prior, R. L., Fang, N., Ronis, M. J., and Badger, T. M. (2005). Isoflavone conjugates are underestimated in tissues using enzymatic hydrolysis. *J. Agric. Food Chem.* **53,** 6858–6863.

Gutendorf, B., and Westendorf, J. (2001). Comparison of an array of in vitro assays for the assessment of the estrogenic potential of natural and synthetic estrogens, phytoestrogens and xenoestrogens. *Toxicology* **166,** 79–89.

Harris, D. M., Besselink, E., Henning, S. M., Go, V. L., and Heber, D. (2005). Phytoestrogens induce differential estrogen receptor alpha- or beta-mediated responses in transfected breast cancer cells. *Exp. Biol. Med. (Maywood)* **230,** 558–568.

Hsieh, C. Y., Santell, R. C., Haslam, S. Z., and Helferich, W. G. (1998). Estrogenic effects of genistein on the growth of estrogen receptor-positive human breast cancer (MCF-7) cells *in vitro* and *in vivo*. *Cancer Res.* **58,** 3833–3838.

Izumi, T., Piskula, M. K., Osawa, S., Obata, A., Tobe, K., Saito, M., Kataoka, S., Kubota, Y., and Kikuchi, M. (2000). Soy isoflavone aglycones are absorbed faster and in higher amounts than their glucosides in humans. *J. Nutr.* **130,** 1695–1699.

Jefferson, W. N., and Newbold, R. R. (2000). Potential endocrine-modulating effects of various phytoestrogens in the diet. *Nutrition* **16,** 658–662.

Kakehashi, A., Ishii, N., Shibata, T., Wei, M., Okazaki, E., Tachibana, T., Fukushima, S., and Wanibuchi, H. (2011). Mitochondrial prohibitins and septin 9 are implicated in the onset of rat hepatocarcinogenesis. *Toxicol. Sci.* **119,** 61–72.

Kinoshita, A., Wanibuchi, H., Morimura, K., Wei, M., Shen, J., Imaoka, S., Funae, Y., and Fukushima, S. (2003). Phenobarbital at low dose exerts hormesis in rat hepatocarcinogenesis by reducing oxidative DNA damage, altering cell proliferation, apoptosis and gene expression. *Carcinogenesis* **24,** 1389–1399.

Klein, C. J., Vrana, J. A., Theis, J. D., Dyck, P. J., Spinner, R. J., Mauermann, M. L., Bergen, H. R., 3rd, Zeldenrust, S. R., and Dogan, A. (2011). Mass spectrometric-based proteomic analysis of amyloid neuropathy type in nerve tissue. *Arch. Neurol.* **68,** 195–199.

Lamartiniere, C. A., Moore, J. B., Brown, N. M., Thompson, R., Hardin, M. J., and Barnes, S. (1995). Genistein suppresses mammary cancer in rats. *Carcinogenesis* **16,** 2833–2840.

Lehmann, L., Jiang, L., and Wagner, J. (2008). Soy isoflavones decrease the catechol-O-methyltransferase-mediated inactivation of 4-hydroxyestradiol in cultured MCF-7 cells. *Carcinogenesis* **29,** 363–370.

Lu, F. C. (1988). Acceptable daily intake: Inception, evolution, and application. *Regul. Toxicol. Pharmacol.* **8,** 45–60.

Lucki, N. C., and Sewer, M. B. (2011). Genistein stimulates MCF-7 breast cancer cell growth by inducing acid ceramidase (ASAH1) gene expression. *J. Biol. Chem.* **286,** 19399–19409.

Maekawa, A., Onodera, H., Tanigawa, H., Furuta, K., Matsuoka, C., Kanno, J., Ogiu, T., and Hayashi, Y. (1986). Spontaneous neoplastic and non-neoplastic lesions in aging Donryu rats. *Jpn. J. Cancer Res.* **77,** 882–890.

Messina, M. J., and Loprinzi, C. L. (2001). Soy for breast cancer survivors: A critical review of the literature. *J. Nutr.* **131,** 3095S–3108S.

Messina, M. J., and Wood, C. E. (2008). Soy isoflavones, estrogen therapy, and breast cancer risk: Analysis and commentary. *Nutr. J.* **7,** 17.

Milanezi, F., Carvalho, S., and Schmitt, F. C. (2008). EGFR/HER2 in breast cancer: A biological approach for molecular diagnosis and therapy. *Expert Rev. Mol. Diagn.* **8,** 417–434.

Mizumoto, Y., Kyo, S., Kiyono, T., Takakura, M., Nakamura, M., Maida, Y., Mori, N., Bono, Y., Sakurai, H., and Inoue, M. (2011). Activation of NF-

Downloaded from http://toxsci.oxfordjournals.org/ at Oska City University - Medical Campus on February 28, 2012

kappaB is a novel target of KRAS-induced endometrial carcinogenesis. *Clin. Cancer Res.* **17,** 1341–1350.

Naaz, A., Yellayi, S., Zakroczymski, M. A., Bunick, D., Doerge, D. R., Lubahn, D. B., Helferich, W. G., and Cooke, P. S. (2003). The soy isoflavone genistein decreases adipose deposition in mice. *Endocrinology* **144,** 3315–3320.

Nakayama, M., Nakajima, D., Nagase, T., Nomura, N., Seki, N., and Ohara, O. (1998). Identification of high-molecular-weight proteins with multiple EGF-like motifs by motif-trap screening. *Genomics* **51,** 27–34.

Nagaoka, T., Onodera, H., Matsushima, Y., Todate, A., Shibutani, M., Ogasawara, H., and Maekawa, A. (1990). Spontaneous uterine adenocarcinomas in aged rats and their relation to endocrine imbalance. *J. Cancer Res. Clin. Oncol.* **116,** 623–628.

Nagaoka, T., Takegawa, K., Takeuchi, M., and Maekawa, A. (2000). Effects of reproduction on spontaneous development of endometrial adenocarcinomas and mammary tumors in Donryu rats. *Jpn. J. Cancer Res.* **91,** 375–382.

Nagaoka, T., Takeuchi, M., Onodera, H., Matsushima, Y., Ando-Lu, J., and Maekawa, A. (1994). Sequential observation of spontaneous endometrial adenocarcinoma development in Donryu rats. *Toxicol. Pathol.* **22,** 261–269.

Reagan-Shaw, S., Nihal, M., and Ahmad, N. (2008). Dose translation from animal to human studies revisited. *FASEB J.* **22,** 659–661.

Seth, A., Kitching, R., Landberg, G., Xu, J., Zubovits, J., and Burger, A. M. (2003). Gene expression profiling of ductal carcinomas in situ and invasive breast tumors. *Anticancer Res.* **23,** 2043–2051.

Song, X., Bandow, J., Sherman, J., Baker, J. D., Brown, P. W., McDowell, M. T., and Molloy, M. P. (2008). iTRAQ experimental design for plasma biomarker discovery. *J. Proteome Res.* **7,** 2952–2958.

Thomas, S. M., Bhola, N. E., Zhang, Q., Contrucci, S. C., Wentzel, A. L., Freilino, M. L., Gooding, W. E., Siegfried, J. M., Chan, D. C., and Grandis, J. R. (2006). Cross-talk between G protein-coupled receptor and epidermal growth factor receptor signaling pathways contributes to growth and invasion of head and neck squamous cell carcinoma. *Cancer Res.* **66,** 11831–11839.

Unfer, V., Casini, M. L., Costabile, L., Mignosa, M., Gerli, S., and Di Renzo, G. C. (2004a). Endometrial effects of long-term treatment with phytoestrogens: A randomized, double-blind, placebo-controlled study. *Fertil. Steril.* **82,** 145–148.

Unfer, V., Casini, M. L., Costabile, L., Mignosa, M., Gerli, S., and Di Renzo, G. C. (2004b). High dose of phytoestrogens can reverse the antiestrogenic effects of clomiphene citrate on the endometrium in patients undergoing intrauterine insemination: A randomized trial. *J. Soc. Gynecol. Investig.* **11,** 323–328.

Wang, L., Kuang, L., Pan, X., Liu, J., Wang, Q., Du, B., Li, D., Luo, J., Liu, M., Hou, A., *et al.* (2010). Isoalvaxanthone inhibits colon cancer cell proliferation, migration and invasion through inactivating Rac1 and AP-1. *Int. J. Cancer* **127,** 1220–1229.

Wang, T. T., Sathyamoorthy, N., and Phang, J. M. (1996). Molecular effects of genistein on estrogen receptor mediated pathways. *Carcinogenesis* **17,** 271–275.

Wunderer, G., Walter, I., Eschenbacher, B., Lang, M., Kellermann, J., and Kindermann, G. (1990). Ile-Ser-bradykinin is an aberrant permeability factor in various human malignant effusions. *Biol. Chem. Hoppe Seyler* **371,** 977–981.

Wuttke, W., Jarry, H., and Seidlova-Wuttke, D. (2007). Isoflavones—safe food additives or dangerous drugs? *Ageing Res. Rev.* **6,** 150–188.

Xiao, C. W. (2008). Health effects of soy protein and isoflavones in humans. *J. Nutr.* **138,** 1244S–1249S.

Yamakoshi, J., Piskula, M. K., Izumi, T., Tobe, K., Saito, M., Kataoka, S., Obata, A., and Kikuchi, M. (2000). Isoflavone aglycone-rich extract without soy protein attenuates atherosclerosis development in cholesterol-fed rabbits. *J. Nutr.* **130,** 1887–1893.

Yoshida, M., Kudoh, K., Katsuda, S., Takahashi, M., Ando, J., and Maekawa, A. (1998). Inhibitory effects of uterine endometrial carcinogenesis in Donryu rats by tamoxifen. *Cancer Lett.* **134,** 43–51.

Young, S., and Hallowes, R. C. (1973). Tumors of the mammary gland. In *Pathology of Tumors in Laboratory Animals-Tumors of the Rat* (V. S. Turusov, Ed.), pp. 31–86. IARC, Switzerland.

Downloaded from http://toxsci.oxfordjournals.org/ at Oska City University - Medical Campus on February 28, 2012

Published OnlineFirst November 11, 2010; DOI:10.1158/1940-6207.CAPR-10-0163

Research Article

Cancer Prevention Research

# Acyclic Retinoid Inhibits Diethylnitrosamine-Induced Liver Tumorigenesis in Obese and Diabetic C57BLKS/J- +Lepr$^{db}$/+Lepr$^{db}$ Mice

Masahito Shimizu[1], Hiroyasu Sakai[1], Yohei Shirakami[1], Junpei Iwasa[1], Yoichi Yasuda[1], Masaya Kubota[1], Koji Takai[1], Hisashi Tsurumi[1], Takuji Tanaka[2], and Hisataka Moriwaki[1]

## Abstract

Obesity and the related metabolic abnormalities are associated with increased risk of hepatocellular carcinoma (HCC). Malfunctioning of retinoid X receptor (RXR) α due to phosphorylation by Ras/MAPK also plays a critical role in liver carcinogenesis. In the present study, we examined the effects of acyclic retinoid (ACR), which targets RXRα, on the development of diethylnitrosamine (DEN)-induced liver tumorigenesis in C57BLKS/J- +Lepr$^{db}$/+Lepr$^{db}$ (*db/db*) obese mice. Male *db/db* mice were given tap water containing 40 ppm DEN for 2 weeks, after which they were fed a diet containing 0.03% or 0.06% of ACR throughout the experiment. In mice treated with either dose of ACR for 34 weeks, the development of liver cell adenomas was significantly inhibited as compared with basal diet-fed mice. ACR markedly inhibited the activation of Ras and phosphorylation of the ERK (extracellular signal-regulated kinase) and RXRα proteins in the livers of experimental mice. It also increased the expression of *RARβ* and *p21$^{CIP1}$* mRNA while decreasing the expression of *cyclin D1*, *c-Fos*, and *c-Jun* mRNA in the liver, thereby restoring RXRα function. Administration of ACR improved liver steatosis and activated the AMPK protein. The serum levels of insulin decreased by ACR treatment, whereas the quantitative insulin sensitivity check index (QUICKI) values increased, indicating improved insulin sensitivity. The serum levels of TNF-α and the expression levels of *TNF-α*, *IL-6*, and *IL-1β* mRNA in the livers of DEN-treated *db/db* mice were decreased by ACR treatment, suggesting attenuation of the chronic inflammation induced by excessive fatty deposits. ACR may be, therefore, useful in the chemoprevention of obesity-related HCC. *Cancer Prev Res; 4(1); 128–36. ©2010 AACR.*

## Introduction

Hepatocellular carcinoma (HCC) is a serious health-care problem worldwide. The risk factors associated with the development of HCC include chronic hepatitis B and/or hepatitis C infection, particularly with subsequent cirrhosis. Recent evidence also indicates that obesity and the related metabolic abnormalities, especially diabetes mellitus, increase the risk of HCC (1–3). In a rodent model, the occurrence of diethylnitrosamine (DEN)-induced liver tumorigenesis was found to be significantly higher in obese and diabetic C57BLKS/J-+Lepr$^{db}$/+Lepr$^{db}$ (*db/db*) mice than in genetic control mice (4). Diabetes mellitus has been shown to increase the risk of primary HCC in patients with viral hepatitis (5). Insulin resistance is also significantly associated with the recurrence of stage I HCC after curative treatment (6). Nonalcoholic fatty liver disease (NAFLD) is a hepatic manifestation of the insulin resistance syndrome, and in a subset of NAFLD patients, the condition progresses to nonalcoholic steatohepatitis, which involves severe inflammation and therefore poses the threat of HCC (7, 8). Coexistent obesity or steatosis exacerbates liver injury and fibrosis and thus is involved in liver tumorigenesis (9). Therefore, patients with obesity and insulin resistance comprise a high-risk group for HCC, and their treatment must target the prevention of this malignancy.

Acyclic retinoid (ACR, the same substance as NIK-333), a synthetic retinoid, apparently exerts chemopreventive effects on the development of HCC (10). It inhibits experimental liver carcinogenesis and suppresses the

**Authors' Affiliations:** [1]Department of Medicine, Gifu University Graduate School of Medicine, Gifu, Japan, and [2]Department of Oncologic Pathology, Kanazawa Medical University, Ishikawa, Japan

**Note:** Supplementary data for this article are available at Cancer Prevention Research Online (http://cancerprevres.aacrjournals.org/).

**Corresponding Author:** Masahito Shimizu, Department of Medicine, Gifu University Graduate School of Medicine, 1-1 Yanagido, Gifu 501-1194, Japan. Phone: 81-(58)-230-6313; Fax: 81-(58)-230-6310; E-mail: shimim-gif@umin.ac.jp

**doi:** 10.1158/1940-6207.CAPR-10-0163

©2010 American Association for Cancer Research.



Downloaded from cancerpreventionresearch.aacrjournals.org on January 25, 2012
Copyright © 2011 American Association for Cancer Research

Published OnlineFirst November 11, 2010; DOI:10.1158/1940-6207.CAPR-10-0163



growth of HCC-derived cells by inducing apoptosis and causing cell-cycle arrest in $G_0$–$G_1$ (11–15). These effects of ACR are associated with its agonistic activity for distinct nuclear retinoid receptors—retinoid X receptors (RXR) and retinoic acid receptors (RAR), both of which have 3 subtypes (α, β, and γ; 16)—and subsequent expression of the ACR target genes *RAR*β and $p21^{CIP1}$ (12–15). A clinical trial revealed that oral administration of ACR significantly reduced the incidence of posttherapeutic HCC recurrence and improved the survival rates of patients (17, 18). A phase II/III trial of ACR confirmed its effectiveness in preventing second primary HCC in hepatitis C virus–positive patients in a large-scale ($n$ = 401) randomized, placebo-controlled trial; hazard ratio for recurrence-free survival with ACR 600 mg/d versus placebo was 0.27 (95% CI, 0.07–0.96) after 2 years randomization (19).

Among the retinoid receptors, RXRα is considered as one of the most important receptors with respect to the regulation of fundamental cell activities because it forms a heterodimer with other nuclear receptors and thereby acts as the master regulator of nuclear receptors (20). Recent studies indicate that phosphorylation of RXRα abolishes its ability to form a heterodimer with RARβ, and the accumulation of phosphorylated RXRα (p-RXRα, i.e., nonfunctional RXRα), which is caused by activation of the Ras/mitogen-activated protein kinase (MAPK)/extracellular signal-regulated kinase (ERK) signaling pathway, plays a critical role in the development of HCC (10, 21, 22). On the other hand, the effects of ACR in suppressing growth and inducing apoptosis in HCC cells depend on the inactivation of Ras-ERK signaling system and subsequent RXRα dephosphorylation (15, 23, 24). In the present study, we examined the effects of ACR on obesity-related liver tumorigenesis by focusing on the inhibition of RXRα phosphorylation. We also examined whether ACR treatment improves the insulin resistance, liver steatosis, and inflammatory condition caused by obesity with DEN-treated *db/db* mice, a useful preclinical model, to evaluate the mechanisms underlying the inhibition of obesity-related liver tumorigenesis by chemopreventive drugs (4).

## Materials and Methods

### Animals and chemicals

Four-week-old male *db/db* mice were obtained from Japan SLC, Inc. All mice received humane care and were housed at Gifu University Life Science Research Center in accordance with the Institutional Animal Care Guidelines. DEN was purchased from Sigma Chemical Co. ACR was supplied by Kowa Pharmaceutical Co.

### Experimental procedure

The experimental protocol, which was approved by the Institutional Committee of Animal Experiments of Gifu University, was as described previously (4). At 5 weeks of age, 40 *db/db* mice were randomly divided into 5 groups. All the mice in groups 1 ($n$ = 10), 2 ($n$ = 10), and 3 ($n$ = 10) were given tap water containing 40 ppm of DEN for the first 2 weeks, which is sufficient to develop liver neoplasms in *db/db* mice (4). After DEN treatment, the mice in groups 2 and 3 were fed the basal diet CRF-1 (Oriental Yeast Co.) containing 0.03% ACR (group 2) or 0.06% ACR (group 3), respectively, with free access to the feed till the end of experiment. Group 4 ($n$ = 5) was fed the CRF-1 diet containing 0.06% ACR. The mice in groups 1 and 5 ($n$ = 5) were fed the CRF-1 diet throughout the experiment. The rationale for the doses (0.03% and 0.06%) selection of ACR was based on previous studies, in which similar doses of ACR inhibited experimental liver carcinogenesis induced by chemical agents (25, 26). At 41 weeks of age (after 34 weeks of ACR treatment), all the mice were sacrificed by $CO_2$ asphyxiation to check for the development of HCC, liver cell adenoma, and foci of cellular alteration (FCA).

### Histopathologic analysis

At sacrifice, the livers were immediately removed and macroscopically inspected for the presence of neoplasms. Maximum sagittal sections of each lobe (6 lobes) were used for histopathologic examination. For all experimental groups, 4-μm thick sections of formalin-fixed, paraffin-embedded livers were stained routinely with hematoxylin and eosin (H&E) for histopathologic examination. The presence of HCC, liver cell adenoma, and FCA was judged according to previously described criteria (27). The multiplicity of FCA was assessed on a per unit area ($cm^2$) basis.

### Ras activation assay

Ras activity was determined using a Ras activation assay kit (Upstate Biotechnology) according to the manufacturer's instructions. Ras was precipitated in equivalent amounts of liver extract (50 μg) from DEN-treated mice (groups 1–3) by using Raf-1/Ras-binding domain-immobilized agarose, which was then subjected to Western blot analysis using anti-Ras antibody (24). The intensity of the blots was quantified using NIH imaging software Version 1.62.

### Protein extraction and Western blot analysis

Total protein was extracted from the nontumor site of livers of DEN-treated mice, and equivalent amounts of proteins (30 μg per lane) were examined by Western blot analysis (4). Previously described primary antibodies for RXRα (ΔN-197 and D-20), ERK, phosphorylated ERK (p-ERK), Stat3, p-Stat3, AMP-activated kinase (AMPK), p-AMPK, and GAPDH were used (15, 22, 28, 29). The ΔN-197 antibody is considered a specific antibody for the p-RXRα protein (22, 23). The GAPDH antibody served as a loading control.



Downloaded from cancerpreventionresearch.aacrjournals.org on January 25, 2012
Copyright © 2011 American Association for Cancer Research

Published OnlineFirst November 11, 2010; DOI:10.1158/1940-6207.CAPR-10-0163



### RNA extraction and quantitative real-time reverse transcription PCR

Total RNA was isolated from the nontumor site livers of DEN-treated mice by using the RNAqueous-4PCR kit (Ambion Applied Biosystems). cDNA was amplified from 0.2 μg of total RNA by using the SuperScript III First-Strand Synthesis System (Invitrogen), and quantitative real-time reverse transcription PCR (RT-PCR) analysis was carried out as described previously (4). The specific primers used for amplification of the *TNF-α*, *IL-6*, *IL-1β*, and *β-actin* genes were as described previously (30). The primers for the amplification of *RARβ*, *p21$^{CIP1}$*, *cyclin D1*, *c-Jun*, and *c-Fos* genes are listed in Supplementary Table S1.

### Clinical chemistry

Before sacrifice, the mice were fasted for 6 hours, and at sacrifice, blood samples were collected for assaying the serum concentrations of insulin, glucose, and TNF-α, which was as described previously (4, 29). The serum TNF-α (Shibayagi) levels were determined using an enzyme immunoassay according to the manufacturer's protocol. Insulin resistance was estimated by determining the quantitative insulin sensitivity check index (QUICKI) as follows: $QUICKI = 1/[\log(I_0) + \log(G_0)]$, where $I_0$ is the fasting insulin level and $G_0$ is the fasting glucose level, which correlates with the glucose clamp method (31).

### Hepatic lipid analysis

Approximately 200 mg of frozen liver was homogenized, and lipids were extracted using Folch's method (32). The levels of triglyceride in the liver were measured using the triglyceride E-test kit (Wako Pure Chemical Co.) according to the manufacturer's protocol. To visualize the intrahepatic lipids, Sudan III staining was conducted using the standard procedure with frozen sections.

### Statistical analysis

The results are presented as the mean ± SD and were analyzed using the GraphPad Instat software program Version 3.05 (GraphPad Software) for Macintosh. Differences among the groups were analyzed by either 1-way ANOVA or, as required, by 2-way ANOVA. When the ANOVA showed a statistically significant effect ($P < 0.05$), each experimental group was compared with the control group by using the Tukey–Kramer multiple comparisons test. The differences were considered significant when the 2-sided $P$ value was less than 0.05.

## Results

### General observations

As shown in Table 1, no significant differences were observed in the body, kidney, and fat weights among the groups at the end of the study. A significant decrease in the liver weight was observed in the ACR-treated groups as compared with the basal diet-fed group ($P < 0.05$ or $P < 0.01$), irrespective of DEN treatment. Histopathologic examination showed the absence of ACR toxicity in the liver, kidney, and spleen (data not shown).

### Effects of ACR on DEN-induced liver tumorigenesis in *db/db* mice

Table 2 summarizes the incidence and multiplicity of liver neoplasms (adenoma and HCC) and FCA in the mice from all groups. FCA developed in the livers of mice from all groups, irrespective of DEN treatment. On the other hand, liver cell adenomas developed only in the DEN-treated *db/db* mice. HCCs also developed in all DEN-treated groups; however, the incidence (10% in each group) wan not high. These findings might be associated with experimental protocol because the duration of the experiments (41 weeks) was sufficient to develop adenoma but not HCC. In mice treated with either dose (0.03% and 0.06%) of ACR, the incidence ($P < 0.01$ in each comparison) and multiplicity of adenoma ($P < 0.05$ or $P < 0.01$) were significantly inhibited compared to ACR-untreated mice. The number of FCA was also significantly decreased by ACR treatment, irrespective of DEN treatment ($P < 0.001$ or $P < 0.05$).

### Effects of ACR on Ras activity and phosphorylation of RXRα, ERK, and Stat3 proteins in the livers of DEN-treated *db/db* mice

ACR prevents the growth of HCC cells by inactivating Ras-ERK and dephosphorylating RXRα, thereby restoring RXRα function (10, 15, 23, 24). Stat3 is also an ACR target for the inhibition of cancer cell growth (28). Therefore, the effects of ACR on the inhibition of Ras activity and phosphorylation of the RXRα, ERK, and Stat3 proteins were examined in this study by using an obesity-related liver tumorigenesis model. As shown in Figure 1A, the activity of Raf-1–bound Ras in the liver was significantly inhibited by treatment with either dose of ACR ($P < 0.01$). The expression levels of the p-ERK and p-RXRα proteins were also decreased by ACR treatment (Fig. 1B), indicating that ACR inhibits the development of obesity-related liver neoplasms, at least in part, by dephosphorylating RXRα and thereby restoring its function. At both doses, ACR also decreased the expression levels of the p-Stat3 protein in the livers of DEN-treated *db/db* mice (Fig. 1B).

### Effects of ACR on the expression levels of RARβ, p21$^{CIP1}$, cyclin D1, c-Fos, and c-Jun mRNA in the livers of DEN-treated *db/db* mice

ACR inhibits the growth of HCC cells by increasing the cellular levels of RARβ and p21$^{CIP1}$ but decreasing the levels of cyclin D1, and these effects might be associated with the restoration of RXRα function (12–15). It also suppresses the growth of cancer cells by inhibiting the activity of AP-1, which comprises the Jun and Fos oncoprotein families (28). Therefore, the effect of ACR on the mRNA levels of these molecules was examined next. As shown in Figure 1C, quantitative real-time RT-PCR analysis indicated that ACR treatment



Downloaded from cancerpreventionresearch.aacrjournals.org on January 25, 2012
Copyright © 2011 American Association for Cancer Research